

FAKULTA STROJNÍ

CZECH TECHNICAL UNIVERSITY

FACULTY OF MECHANICAL ENGINEERING

Department of Process engineering

CFD SIMULATION OF FLOW IN FISH TANKS

Master Thesis

PRASHANT N

NAME OF THE SUPERVISOR: Ing. Karel Petera, Ph.D.

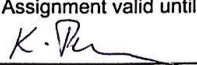
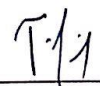
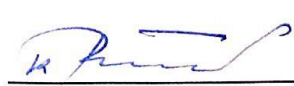


MASTER'S THESIS ASSIGNMENT

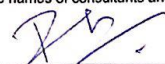
I. Personal and study details

| | | | |
|-------------------------|--|---------------------|---------------|
| Student's name: | N Prashant | Personal ID number: | 464045 |
| Faculty / Institute: | Faculty of Mechanical Engineering | | |
| Department / Institute: | Department of Process Engineering | | |
| Study program: | Mechanical Engineering | | |
| Branch of study: | Process Engineering | | |

II. Master's thesis details

| | | | |
|---|---|---|-------------------|
| Master's thesis title in English: | CFD simulation of flow in fish tanks | | |
| Master's thesis title in Czech: | CFD simulation of flow in fish tanks | | |
| Guidelines: | <ul style="list-style-type: none">- Make a literature review of frequently used flow configurations in fish tanks.- Summarize suitable CFD methods and models describing the flow field in fish tanks including the sedimentation of solid particles.- Create a model of the given geometry in ANSYS CFD.- Perform numerical simulations and compare the results with available experimental data.- Summarize the methodology used in the thesis and propose possible improvements of the solution procedure. | | |
| Bibliography / sources: | | | |
| Name and workplace of master's thesis supervisor: | Ing. Karel Petera, Ph.D., Department of Process Engineering, FME | | |
| Name and workplace of second master's thesis supervisor or consultant: | | | |
| Date of master's thesis assignment: | 23.10.2018 | Deadline for master's thesis submission: | 11.01.2019 |
| Assignment valid until: | | | |
|  |  |  | |
| Ing. Karel Petera, Ph.D. Supervisor's signature | prof. Ing. Tomáš Jirout, Ph.D. Head of department's signature | prof. Ing. Michael Valášek, DrSc. Dean's signature | |

III. Assignment receipt

| | |
|---|---|
| The student acknowledges that the master's thesis is an individual work. The student must produce his thesis without the assistance of others, with the exception of provided consultations. Within the master's thesis, the author must state the names of consultants and include a list of references. | |
| <u>30.10.2018</u> Date of assignment receipt |  Student's signature |

Declaration

I hereby declare that I have completed this thesis entitled **CFD simulation of flow in fish tanks** independently with my supervisor and I have attached a full list of references and citations.

I don't have a convincing reason within the meaning of section 60 of the Act No. 121/2000 Coll on copyright, rights related to copyright and amending some laws (copyright act)

In.... Prague....Date.....

.....

Acknowledgement

Firstly, I would like to express my sincere gratitude to my supervisor Ing Karel Petera, Ph.D. for his amazing support and guidance throughout the work of my thesis. Thanks for his patience, motivation and immense knowledge. His guidance helped me, and I have learned a lot from him.

In addition, I would like to thank Ing. Stepan Papacek, Ph.D. for his inputs in thesis work. It helped me fruitfully during the course of my thesis work.

Most importantly I would like to thank my parents for their love they have showered upon me. I would give a special thanks to my father for his additional inputs in my thesis.

ABSTRACT

The aim of this work is to study the hydrodynamics of the fish tanks by analyzing flow patterns through conical fish tank for the appropriate breeding of the fishes. Analyzing flow patterns is imperative in aquaculture tanks in ensuring better breeding of the fishes and attaining better muscle tone for the quality of the fishes. Here for the analysis the primary tool that has been used is CFD (computational fluid dynamics). For finding out the appropriate velocity and flow rates we have used various turbulence models (such as k-epsilon and k- ω models) as a comparative element. We have also tried to establish residence time distribution analysis by comparing various tank designs (such as circular, rectangular and conical tank) by implementing discrete phase models in those tank designs.

Keywords: Conical fish tank, K-epsilon, K-omega, Average velocity, discrete phase model, Residence time distribution.

Table of Contents

| | |
|---|------|
| ABSTRACT..... | v |
| LIST OF TABLES..... | vii |
| LIST OF FIGURES..... | viii |
| CHAPTER 1: INTRODUCTION | 1 |
| 1.1: RECIRCULATING AQUACULTURE SYSTEMS: | 3 |
| 1.1.1 ADVANTAGES OF RECIRCULATING AQUACULTURE SYSTEMS: | 4 |
| CHAPTER 2: OBJECTIVES AND MOTIVATION..... | 5 |
| CHAPTER 3: EXPERIMENTAL SET UP | 6 |
| 3.1: SETTING UP THE REARING UNITS | 6 |
| 3.2: EXPERIMENTAL DATA AND CALCULATION | 8 |
| CHAPTER 4: GEOMETRICAL DESCRIPTION OF THE FISH TANK..... | 11 |
| CHAPTER 5: ANSYS MESHING AND METHODS USED IN MY THESIS WORK..... | 14 |
| 5.1: MESH QUALITY | 15 |
| 5.2: ILLUSTRATION OF THE MESH FOR THE PROPOSED CONICAL TANK DESIGN AND THE MESH QUALITY | 16 |
| 5.3 GRID CONVERGENCY STUDY | 18 |
| CHAPTER 5: INTRODUCTION TO CFD (COMPUTATIONAL FLUID DYNAMICS ANF ITS METHODS) AND ITS WORKING TECHNIQUES..... | 23 |
| 5.1: CFD WORK CODES (principles) | 24 |
| 5.2: GOVERNING EQUATIONS AND ITS FORMS: | 26 |
| CHAPTER 6: TURBULENCE AND ITS MODELS DESCRIPTION. | 28 |
| 6.1: TURBULENCE FLOW CALCULATIONS: | 29 |
| CHAPTER 7: RESULTS AND DISCUSSION..... | 35 |
| 7.1: CFD MODEL TO PROBLEM SOLUTION | 35 |
| 7.2: RESULTS AND COMPARISON | 38 |
| 7.3: DISCRETE PHASE MODELS | 48 |
| 7.3.1: RESIDENCE TIME DISTRIBUTION | 50 |
| CHAPTER 8: CONCLUSION AND FUTURE WORK RECOMMENDATIONS..... | 53 |
| 8.1: FUTURE PROSPECTS OF THE WORK | 54 |
| REFERENCES:..... | 55 |
| APPENDICES:..... | 56 |

LIST OF TABLES

| | |
|---|----|
| <i>Table 1: Experimental data</i> | 8 |
| <i>Table 2: the calculated values by generating the MATLAB SCRIPT</i> | 21 |
| <i>Table 3: experimental vs simulated (spallart almaras)</i> | 40 |
| <i>Table 4: experimental vs simulated (k epsilon realizable)</i> | 41 |
| <i>Table 5: experimental vs simulated(k epsilon realizable)</i> | 42 |
| <i>Table 6: experimental vs simulated (k epsilon realizable)</i> | 43 |
| <i>Table 7: representation of the k omega model(SST)</i> | 44 |
| <i>Table 8: experimental vs simulated (k-omega SST)</i> | 45 |
| <i>Table 9: experimental vs simulated (k-epsilon realizable)</i> | 46 |
| <i>Table 10: The average velocities are calculated for the mesh elements (173,882).</i> | 47 |
| <i>Table 11: The average velocities are calculated for the mesh elements (397,396)</i> | 47 |
| <i>Table 12: The average velocities are calculated for the mesh elements (900,515)</i> | 47 |
| <i>Table 13: residence time distribution of conical tank</i> | 51 |
| <i>Table 14: residence time distribution of the circular tank</i> | 52 |
| <i>Table 15: residence time distribution of the rectangular tank</i> | 52 |

LIST OF FIGURES

| | |
|---|----|
| Figure 1:representation of circular tank(pentaires,2018) | 2 |
| Figure 2:representation of rectangular tank(fiber glass industries,2018) | 3 |
| Figure 3:schematic diagram of RAS system(Andrew Forsythe,2018) | 4 |
| Figure 4: typical velocimeter(elsciolab,2018) | 8 |
| Figure 5: illustration of the points where the velocity was calculated | 9 |
| Figure 6:dimensional representation of the model of the fish tank | 11 |
| Figure 7: outlet of the tank (ANSYS 18.2) | 12 |
| Figure 8: conical tank view (ANSYS 18.2) | 12 |
| Figure 9: central hollow tube through the tank | 13 |
| Figure 10:mesh quality recommendations(ANSYS TRAINING MATERIALS,2018) | 15 |
| Figure 11:representation of the mesh | 16 |
| Figure 12:representation of skewness and orthogonal quality | 16 |
| Figure 13: representation of skewness and orthogonal quality | 17 |
| Figure 14:representation of monitored quantity and mesh size | 18 |
| Figure 15: graph representing average velocity vs number of mesh (1-2-3 from left to right) | 22 |
| Figure 16: A typical representation of the turbulent flow and laminar flow (Esfscience,2012) | 29 |
| Figure 17:representation of instantaneous velocity and time average velocity(ANSYS TRAINING MATERIALS,2018) | 32 |
| Figure 18: Illustration of the tank for the y plus | 33 |
| Figure 19: representation of Spallart Almaras model | 38 |
| Figure 20: representation of k epsilon model | 40 |
| Figure 21:representation of k epsilon model(realizable) | 41 |
| Figure 22:representation of k epsilon(realizable) | 43 |
| Figure 23: representation of the k-omega (SST) | 44 |
| Figure 24: representation of the k-omega SST | 45 |
| Figure 25: representation of the k epsilon standard wall | 46 |

CHAPTER 1: INTRODUCTION

The demand of food is increasing at a rapid rate year after year as the population is increasing which is already at 7 billion. With the increasing population the people's dependency on food is also increasing at a rapid rate. One of the most important crises the world is facing now is the pollution. The pollution is increasing at all aspects of life whether its industrial pollution, air pollution, marine pollution etc.

The experiments have been performed in a pollution free environment. Small scale fisheries and aquaculture make critical contributions to development with over 41 million people worldwide, the vast majority of whom live in developing countries working in fish production with fish constituting an important source of nutrient for the poor and often being the cheapest form of animal protein. The countries which has its large chunk of the human population dependent on marine environment either for food purposes. It's imperative for those countries to design and optimize better conditions for the exact breeding of the fishes in the fish tanks.

Aquaculture production units should be designed to create a restricted volume in which aquatic organisms can be reared under the best possible conditions for growth. To make aquaculture compatible with environmental restrictions and with other important economic activities such as tourism, fishing, tanks must guarantee fish welfare, minimize resource consumption (feed, labor, energy) cause minimal environmental impact and occupy the smallest area possible.

The fish tank design in the fisheries are one of the most important parameters in the fisheries industry. At the same time optimal boundary conditions such as flow parameters specially velocity profiles for the fish tanks are also imperative in ensuring the breeding of the fishes in the fisheries especially maintaining fish health, muscle tone and respiration. In this study we have tried our best to design velocity profiles and flow rates and compare them with experimental data which might present the conditions for the optimal breeding of the fishes.

There are a variety of tank designs which are of standard use in aquaculture systems. These include Round tanks or circular tanks, rectangular tanks. Round tanks have the advantage of a naturally self-cleaning action and provide a uniform flow pattern for fishes. As the water swirls around the tank, solids are drawn towards the middle, where the outlet is situated.

Due to this property, they are often used in hatcheries, where due to high feed rates, solids loadings (waste feed and feces) can be very high and in recirculation systems, to remove the solids as soon as possible, before they break down. Raceway is a general term given to a straight sided artificial channel in which fish are held. Generally, these have a high-water turnover rate, occurring in less than one hour. These tanks can be constructed from materials such as fiberglass and concrete.

But we have primarily focused on conical fish tanks and compared a few turbulence models which would give us adequate optimization results for the optimal breeding of the fishes in the tanks.

Typical representation of a circular tank and a rectangular tank are shown in figures 1 and figure 2.



Figure 1:representation of circular tank (pentaires,2018)

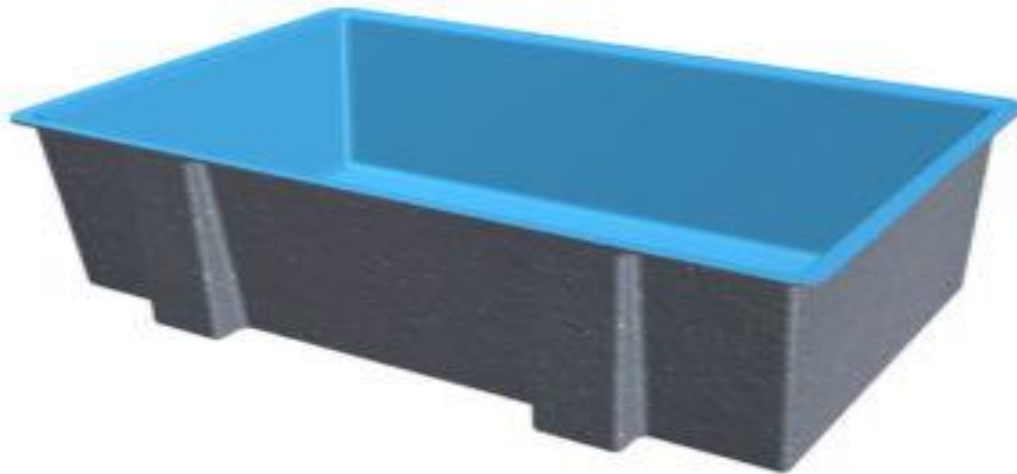


Figure 2:representation of rectangular tank (fiber glass industries,2018)

1.1: RECIRCULATING AQUACULTURE SYSTEMS:

Represents a new and unique way to farm fish. Instead of the traditional method of growing fish outdoors in open ponds and raceways, this system rears fish at high densities, in indoor tanks with a "controlled" environment. Recirculating systems filter and clean the water for recycling back through fish culture tanks (Helfrich and Libey, 2018). New water is added to the tanks only to make up for splash out and evaporation and for that used to flush out waste materials. In contrast, many raceway systems used to grow trout are termed "open" or "flow through" systems because all the water makes only one pass through the tank and then is discarded.

The aquaculture industry, today, focuses on increased production (European Aquaculture Technology and Innovation Platform, 2012), utilizes large rearing units during the early life of fishes i.e. the hatcheries later for pre-growing and on growing. Mediterranean hatcheries use tanks ranging from 2 to 20 m³ in volume for larval rearing, and there is no expectation of significant changes in the future. For weaning and peagrowing, open or closed systems, 10–20m³ raceways or circular tanks are used. On growing is mainly performed in net-pen sea cages of volumes varying between 10000 and 20000m³ (K Lika et al ,2015) but there is a tendency for at two to three-fold increase. In such conditions, the validity and applicability of the research results are questionable.

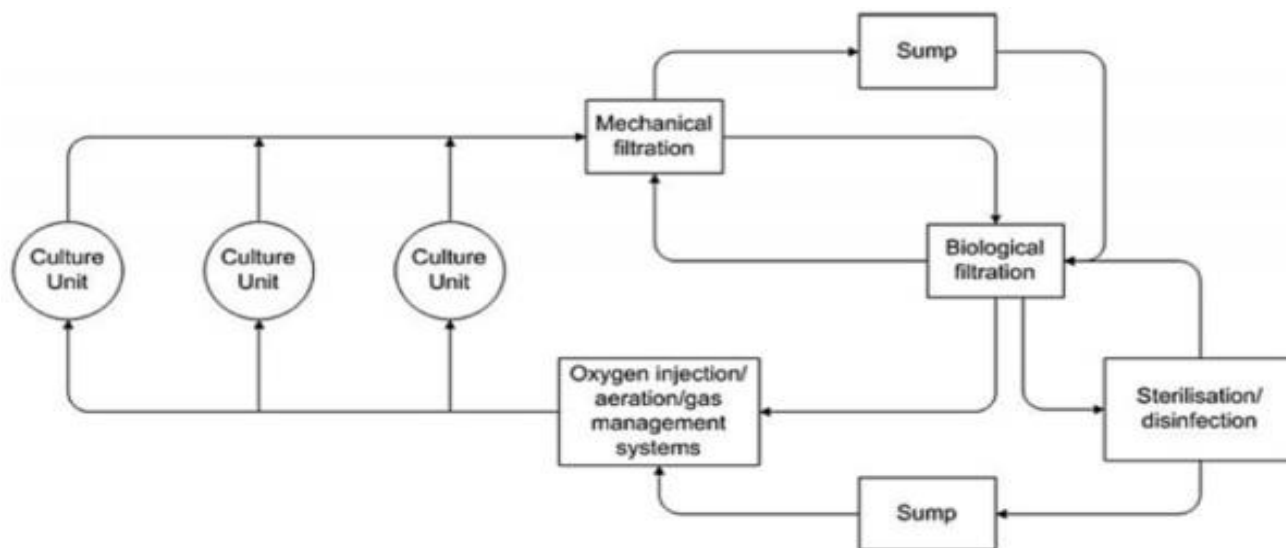


Figure 3:schematic diagram of RAS system (Andrew Forsythe,2018)

RAS system offers the advantage that the temperature and other variables can be controlled in order to maximize growth and maintain fish health to a large extent. RAS system also requires much less incoming water some newer plants require only approx. 1-5% (Forsythe,2018) compared to flow through farms minimizing discharge to environment even when the water supplies are quite minimal.

1.1.1 ADVANTAGES OF RECIRCULATING AQUACULTURE SYSTEMS:

- Reduced water requirements as compared to pond aquaculture systems (Martins, New developments in recirculating aquaculture systems, November ,2015).
- Reduced land needs due to high stocking density (Helfrich, fish farming in recirculating aquaculture systems, August ,2015).
- Reduction in waste water effluent volume.

CHAPTER 2: OBJECTIVES AND MOTIVATION

Aquaculture research cover a wide range of experimental methods and research which includes to study the biology of the octa -genic phase cycle of the fish production. Large water enclosures of various kinds are studied and validated with the experimental methods where the flow rate is taken as a parameter especially inlet flow rate of the fish tanks is considered as the primary parameter to obtain the valid data.

To determine optimum parameter, large scale experiments and also small-scale experiments can also be performed but the advantage of the small-scale experiments over large scale is we require smaller number of animals and also the space required is minimal therefore cost effective and also, we can get better results in a shorter period of time.

In this work the primary objective is to study the hydrodynamics of fish tanks. The hydrodynamics of the fish tanks can be studied by establishing various techniques such as calculating velocity at different points in the fish tanks using velocity probes such as acoustic doppler velocimetry. In this work several simulations were performed within the required turbulence model to obtain optimum velocity profile for the fish production in the large water enclosures to ensure proper health for the fishes and optimum conditions for its growth .We have also compared results with respect to the experiment performed in Crete, Greece with reference to the journal published (K Lika et al,2015).

Also, analyzing of the fish feed pellets distribution in the fish tanks has been studied and analyzed by establishing discrete phase models and evaluating residence time distribution in the concerned fish tank.

To determine the optimum flow rate and residence time distribution several analysis methods are proposed but we have developed a CFD (Computational fluid dynamics) model for the calculation for the respective parameter. Through the performance of the analysis we can determine optimum conditions for the breeding of the fishes in the fish tanks.

CHAPTER 3: EXPERIMENTAL SET UP

The experiments (K Lika et al,2015) were performed at the Institute of the marine biology biotechnology and the Hellenic center of the aquaculture research in Crete, Greece. The eggs were originated from the single spawn of larvae where 110 larvae l⁻¹ was achieved in each tank.

There were three tanks of different volumes were used 40,500,2000 liters. Then after 55 days post hatching the juveniles were transferred to 10 m³ tanks for pre-growing.

During the entire experimental period, larvae were held at mean \pm S.D(standard deviation) water temperature of 18.0 \pm 1.6° C, dissolved oxygen (DO) of 7.2 \pm 0.8 mg l⁻¹(milligrams per liter), constant salinity of 36 and pH of 7.9 \pm 0.3. During hatching and until mouth-opening, tanks were kept in complete darkness; a 12D:12L photoperiod regime (lights went on for 8 hours) was applied during the remainder of the experiment. Following mouth-opening and eye development, larvae were exposed to low light intensity conditions (510lx) in the absence of food for a period of 2–4 days to ensure normal swim bladder inflation, while the water surface was also kept free from any oily film using an air-blower skimmer.

Measurements of environmental variables (temperature, DO, pH, NH⁺ and light intensity) were taken daily from all tanks. Total length (LT) measurements were performed daily, while wet mass (MW) was recorded every third day. At the end of the experiment, a sample of 50 individuals from each tank were measured for LT and MW. The total population in each tank and the survival rate were evaluated by counting the total number of individuals. The quality of the individuals in terms of developmental anomalies was evaluated. Sedimented rotifer, phytoplankton and dead larvae were removed regularly.

3.1: SETTING UP THE REARING UNITS

The whole experimental set-up consisted of six 40-liter tanks, four 500-liter tanks and three 2000-liter tanks. The tanks, using a closed water system supported by biological filters, were organized in triplicates (40 and 2000 liter) or in duplicates (500 liter). The volume of the biological filter was 1m³ for every six 40l or two 500l tanks, and 2m³ for every three 2000-liter tanks. Rearing systems were initially filled with filtered borehole water of 36 salinity.

STEP BY STEP PROCEDURE FOR THE EXPERIMENTAL SETUP

- Water, for water renewal, was circulated in all cases from the bottom of the tank through the biological filter using an electric pump. Water circulation rate used to vary during rearing depending on the developmental stage of the larvae.
- In the 40- and 500-liter tanks, the water circulation rate was $5\% \text{ h}^{-1}$ at the beginning and increased to $50\% \text{ h}^{-1}$ while in the 2000l tanks, it was $10\% \text{ h}$ per hour and increased to $100\% \text{ h}$ per hour.
- A second circulation loop was applied individually for each of the 40- and 500-liter tanks, using an air-lift pump to maintain proper hydraulic conditions for rearing.
- The rate of circulation was initially at $5\% \text{ h}^{-1}$ of the water volume and increased gradually to $50\% \text{ h}^{-1}$. This way similar hydraulic conditions were achieved for all conditions.
- Aeration was also provided by means of a wooden diffuser located in the tank center at a rate of 30, 180- and 250-ml min^{-1} for the 40, 500- and 2000-liter tanks.
- Current measurements were performed using a Vectrino velocimeter.

Note: The above data and the content has been referred to the research paper – (K Lika et al, 2015).

The Vectrino velocimetry is high resolution acoustic velocimeter used to measure three-dimensional water velocity in a wide variety of applications from laboratory to the ocean.

Velocimetry:

One of the major aspects of studying tank hydrodynamics is to study about the flow fields in the fish tanks. This could be performed by establishing various techniques such as acoustic doppler velocimetry. ADV (acoustic doppler velocimetry) is one of the modern methods to determine water velocity in fish tanks. One cardinal point that must be considered while performing the experiments the fishes are not taken into consideration or the fishes are not present in the tank while performing these experiments cause these measurements could harm the fishes and affect the hydrodynamics of the fish tanks.

The velocimeter is an instrument that has been used to determine velocity in three-dimensional region. Typical image of a simple velocimeter has been shown in a figure below.

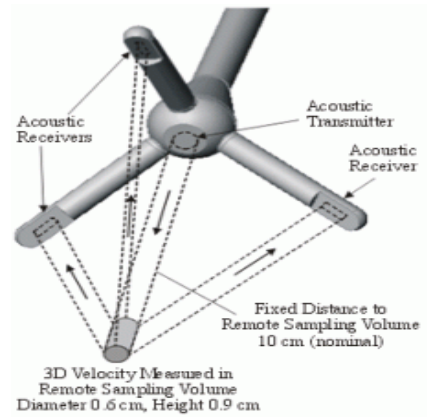


Figure 4: typical velocimeter(elsciolab,2018)

3.2: EXPERIMENTAL DATA AND CALCULATION

| Sl.no | Angle | distance (cm) | x | y | z | U _x (m/s) | U _y (m/s) | U _{z1} (m/s) | U _{z2} (m/s) | U _z (m/s) | U (overall) |
|-------|--------|------------------|-----|-----|----|-------------------------|-------------------------|--------------------------|--------------------------|-------------------------|----------------|
| 1 | 0-180 | 25 | 45 | 0 | 25 | 3.90E-3 | 1.41E-3 | -1.72E-3 | -1.70E-3 | -1.71E-3 | 2.25E-3 |
| 2 | 90-270 | 25 | 0 | -45 | 25 | -4.74E-4 | 2.44E-3 | 7.78E-3 | 7.87E-3 | 7.83E-3 | 9.47E-3 |
| 3 | 0-180 | 25 | 45 | 0 | 25 | -3.66E-3 | 5.30E-4 | 4.47E-3 | 4.56E-3 | 4.52E-3 | 5.84E-3 |
| 4 | 90-270 | 25 | 0 | 45 | 25 | 1.43E-3 | -3.86E-3 | 4.94E-3 | 5.05E-3 | 4.99E-3 | 6.46E-3 |
| 5 | 0-180 | 30 | -25 | 0 | 30 | 1.27E-3 | 9.40E-5 | 1.66E-3 | 1.61E-3 | 1.63E-3 | 2.07E-3 |
| 6 | 90-270 | 30 | 0 | -25 | 30 | 2.23E-3 | 3.06E-3 | -3.54E-3 | -3.70E-3 | -3.62E-3 | 5.24E-3 |
| 7 | 0-180 | 30 | -10 | 0 | 30 | 2.10E-3 | -3.17E-3 | 4.21E-3 | -4.20E-3 | -4.2E-3 | 5.67E-3 |
| 8 | 90-270 | 30 | 0 | -10 | 30 | -1.30E-3 | 4.06E-3 | -2.13E-3 | -2.13E-2 | -2.1E-2 | 2.17E-3 |
| 9 | 0-180 | 30 | 10 | 0 | 30 | -2.10E-3 | 2.77E-3 | -4.90E-3 | -4.95E-3 | -4.93E-3 | 6.05E-3 |
| 10 | 90-270 | 30 | 0 | 10 | 30 | 4.50E-3 | 1.25E-3 | -7.77E-3 | -7.89E-3 | -7.83E-3 | 9.12E-3 |
| 11 | 0-180 | 30 | 25 | 0 | 30 | -3.35E-3 | 3.04E-4 | -4.64E-3 | -4.56E-3 | -4.60E-3 | 5.69E-3 |
| 12 | 90-270 | 30 | 0 | 25 | 30 | 5.81E-3 | -2.97E-3 | -1.13E-3 | -1.19E-3 | -1.16E-3 | 6.62E-3 |

Table 1: Experimental data

I am giving some brief description of the columns and how some of the values are calculated in the experimental data table.

ANGLE: Represents the angular dimension where the velocimeter was kept and calculated experimentally.

DISTANCE: Represents the distance from the bottom of the fish tank where the velocity was calculated represented in centimeters.

X, Y, Z: Represents the coordinates of the points where the velocity was calculated.

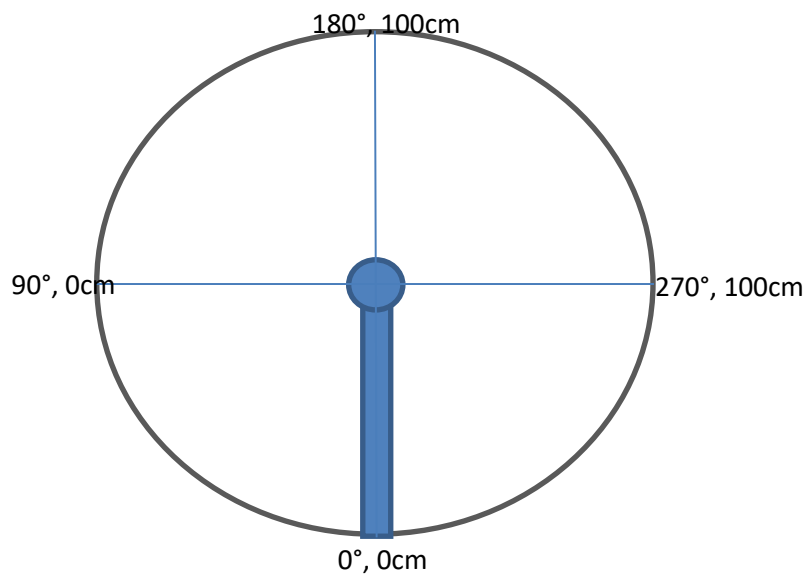


Figure 5: illustration of the points where the velocity was calculated

U_x (m/s): calculated velocity with respect to the x coordinate.

U_y (m/s): calculated velocity with respect to the y coordinate

U_z (m/s): calculated average velocity with respect to z coordinate

$U_{(overall)}$ (m/s): magnitude of the velocity in all the coordinates or dimensions

Here is a brief description of the calculation that is done to determine the velocity magnitude.

The basic formula that can be defined to calculate the velocity is to calculate $U_{(overall)}$

$$U_{(\text{overall})} = \sqrt{U_X^2 + U_Y^2 + U_Z^2}$$

U_Z is calculated by the average of U_{z_1} and U_{z_2} which means

$$U_z = \frac{U_{z_1} + U_{z_2}}{2}$$

Hence the tabular data is generated by calculation of these velocities.

These experimental set up and the description of the procedure for evaluating various parameters are described in the (Journal of fish biology,2015).

(The experimental technique was employed by J.Hanak in his master thesis work (J.Hanak, CFD simulation of flow in fish tanks, CTU in Prague, 2016)

CHAPTER 4: GEOMETRICAL DESCRIPTION OF THE FISH TANK

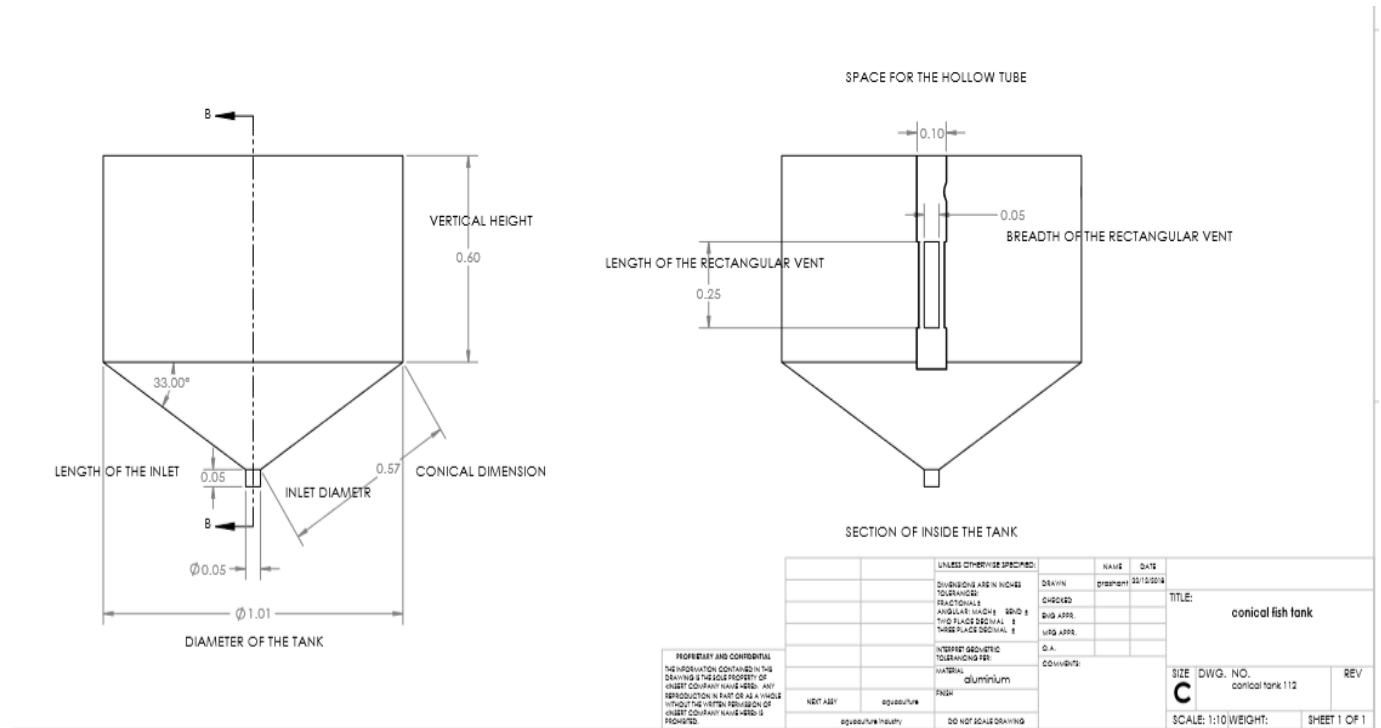


Figure 6:dimensional representation of the model of the fish tank

Here is a brief description of the fish tank designed and the above drafting was done in SOLIDWORKS for better representation.

- Diameter of the tank: 1 m
- Vertical height of the tank: 0.60 m
- Length of the inlet: 0.05m
- Diameter: 0.05m
- Angle of the conical region with respect to the bottom of the tank: 57°
- Conical length of the tank: 0.60m
- Diameter of the hollow tube: 0.10m
- Length of the hollow tube: 0.62m
- Length of the rectangular vent for the hollow tube: 0.25m
- Breadth of the rectangular vent for the hollow tube: 0.05m
- Outlet of the tank(length): 0.05m

- Volume of the fish tank 500 Liters

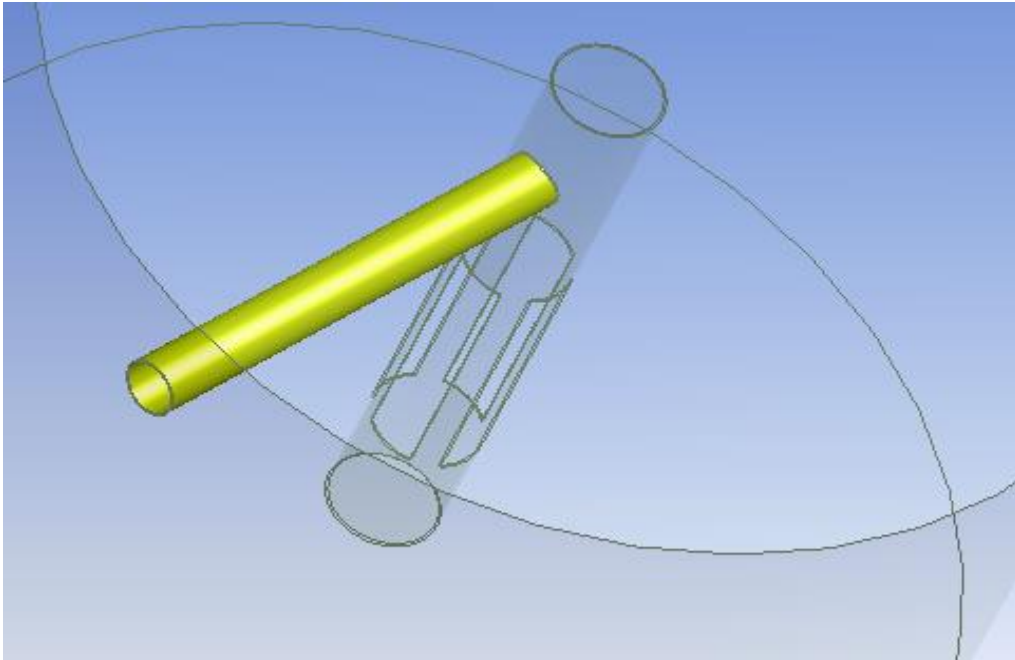


Figure 7: outlet of the tank (ANSYS 18.2)

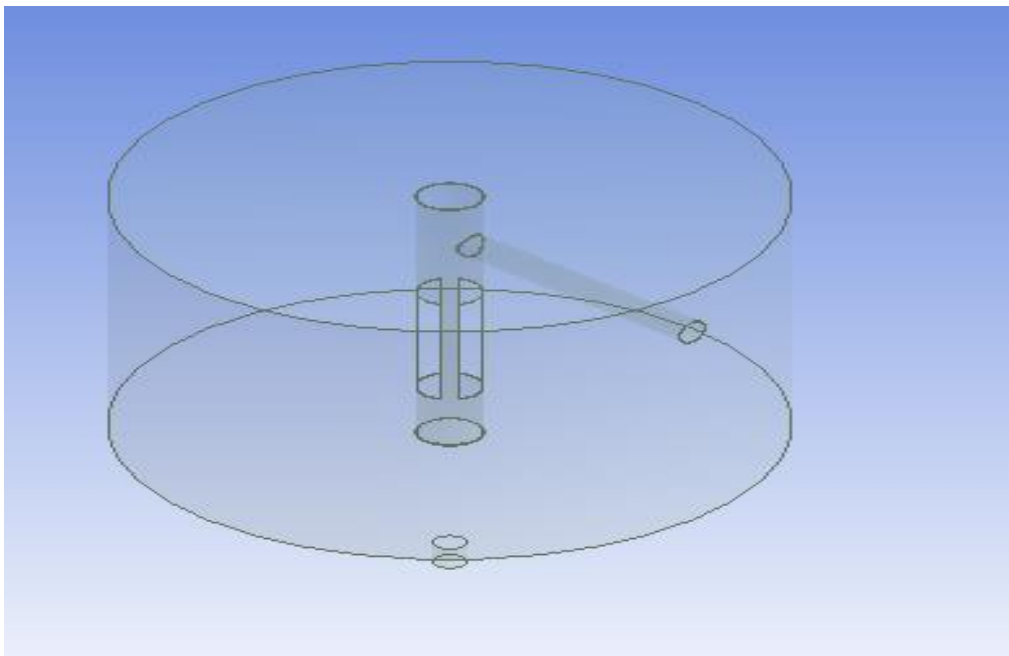


Figure 8: conical tank view (ANSYS 18.2)



Figure 9: central hollow tube through the tank

Note: The net around the tube was used to prevent small fish (larvae) being flooded out of the tank.

CHAPTER 5: ANSYS MESHING AND METHODS USED IN MY THESIS WORK

ANSYS meshing is a method where the geometry is divided into smaller number of elements to create a computational domain. It's one of the important constituents of ANSYS workbench. It helps to create a computational domain which can be transferred to the fluent solver to perform some simulations and compare with some results.

Some of the requirements for meshing are

- Efficiency and accuracy
- Quality

Methods

There are various types of methods that can be used in ANSYS meshing which depends on choice and geometry. Meshing can be made by combining one or more methods.

One of the major methods that has been used (for complex geometries) in ANSYS meshing is tetrahedron methods. In tetrahedron method itself we can divide into two major subsections which are

- Patch conforming
- Patch independent

We have focused mainly on **patch conforming** in this work of thesis.

Patch conforming

It's a bottom up approach which can be described in simple terms such as volumes to faces to edges. Its suitable for good quality CAD geometries. In this method more, details are captured signifying more details are shown in this method.

Patch independent:

It's a top down approach where the volumes are first meshed then the faces and then the edges. Its suitable for poor quality geometries. In this method the details that are captured are less symbolizing therefore less details are shown in patch independent.

5.1: MESH QUALITY

Mesh quality is also another important parameter which defines your mesh and your convergence criteria. It also defines the stability and accuracy of your numerical computation. Regardless the type of mesh that you are using the quality of the mesh is very essential.

Because a bad quality mesh can have some convergence problems and diffused solution.

For stating mesh quality, we use two different types of approaches though there are several approaches such as aspect ratio, Jacobian, parallel deviation etc.

But we primarily focus on determining only two types of approaches which are

- Orthogonal
- Skewness

Low orthogonal and high skewness are not recommended try to keep minimum orthogonal quality >0.1 and for skewness <0.95 . These values may change depending upon the physics and the location of the cell.

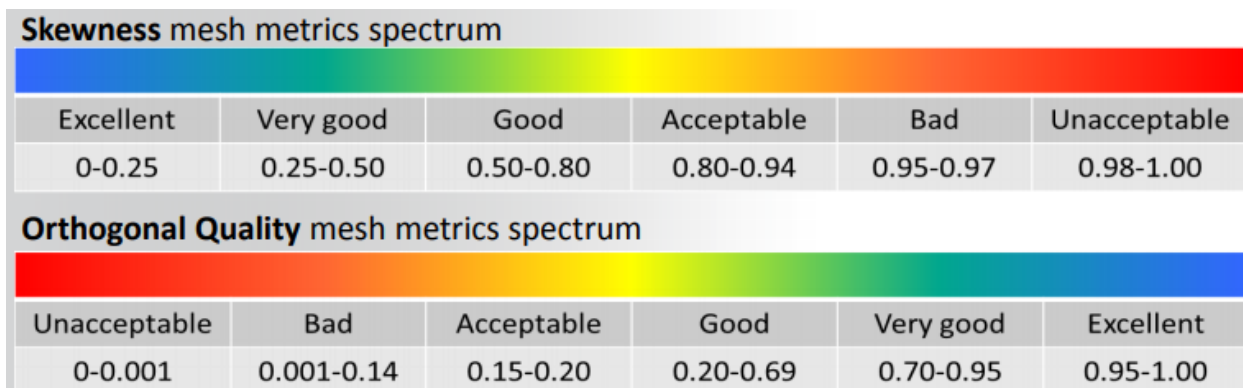


Figure 10: mesh quality recommendations (ANSYS TRAINING MATERIALS,2018)

5.2: ILLUSTRATION OF THE MESH FOR THE PROPOSED CONICAL TANK DESIGN AND THE MESH QUALITY

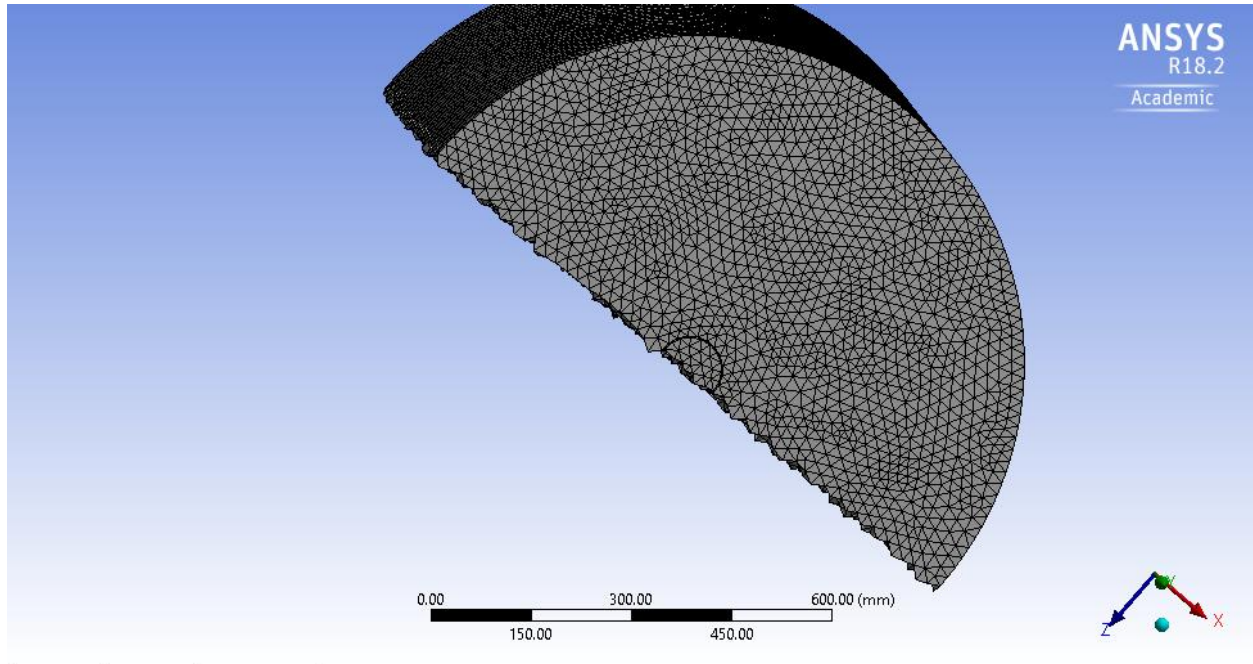


Figure 11: representation of the mesh

Mesh quality:

| | |
|---|-------------|
| Smoothing | Medium |
| Mesh Metric | Skewness |
| <input type="checkbox"/> Min | 5.7689e-007 |
| <input type="checkbox"/> Max | 0.86136 |
| <input type="checkbox"/> Average | 0.21428 |
| <input type="checkbox"/> Standard Deviation | 0.11983 |
| + Inflation | |
| + Assembly Meshing | |
| + Advanced | |

| | |
|---|--------------------|
| Smoothing | Medium |
| Mesh Metric | Orthogonal Quality |
| <input type="checkbox"/> Min | 0.13864 |
| <input type="checkbox"/> Max | 0.99674 |
| <input type="checkbox"/> Average | 0.78415 |
| <input type="checkbox"/> Standard Deviation | 0.11789 |
| + Inflation | |
| + Assembly Meshing | |
| + Advanced | |

Figure 12: representation of skewness and orthogonal quality

The above figure shows the mesh quality for the mesh elements (397,396)

| | |
|---|--------------------|
| <input type="checkbox"/> Target Skewness | Default (0.900000) |
| Smoothing | Medium |
| Mesh Metric | Skewness |
| <input type="checkbox"/> Min | 5.3494e-007 |
| <input type="checkbox"/> Max | 0.85043 |
| <input type="checkbox"/> Average | 0.20838 |
| <input type="checkbox"/> Standard Deviation | 0.11658 |

| Mesh Metric | Orthogonal Quality |
|---|--------------------|
| <input type="checkbox"/> Min | 0.14957 |
| <input type="checkbox"/> Max | 0.99636 |
| <input type="checkbox"/> Average | 0.79016 |
| <input type="checkbox"/> Standard Deviation | 0.11482 |

| |
|--------------------|
| + Inflation |
| + Assembly Meshing |
| + Advanced |
| - Statistics |

Figure 13: representation of skewness and orthogonal quality

The above figure shows us the skewness and orthogonal quality for the mesh elements (900,515).

Both the figures show that the quality of the mesh is good and acceptable.

5.3 GRID CONVERGENCY STUDY

The dependency on the solution on the number of mesh elements is given by the following equation

$$\Phi = \Phi_{ext} + a.N^{-p/d}$$

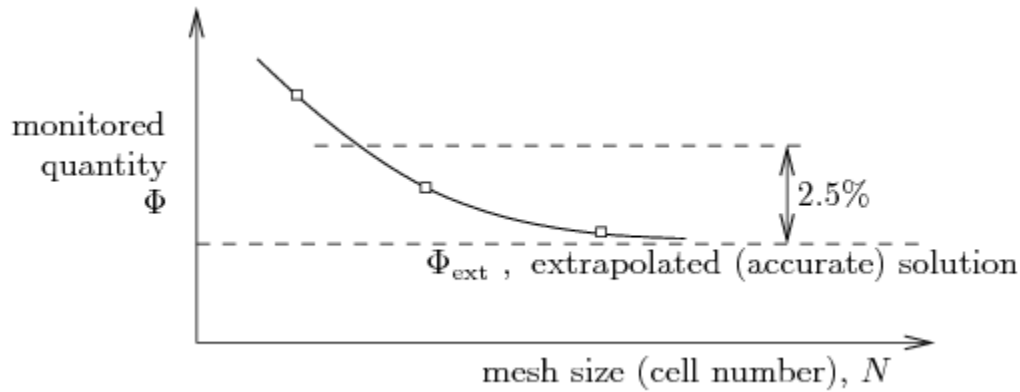


Figure 14:representation of monitored quantity and mesh size

As explained in the figure Φ is the monitored quantity while Φ_{ext} is the extrapolated value and N represents the number of mesh elements. The number of mesh elements powered $-1/D$ represents the dimensional part of the quantity which signifies D is equal to 2 when it is two dimensional and it is equal to 3 when it is three dimensional. So basically, we have three unknown parameters Φ , p and a . hence we can define three different equations with respect to the different elements sizes.

$$\Phi - \Phi_{ext} = a.N_1^{-\frac{1}{D}} \quad (1)$$

$$\Phi - \Phi_{ext} = a.N_2^{-\frac{1}{D}} \quad (2)$$

$$\Phi - \Phi_{ext} = a.N_3^{-\frac{1}{D}} \quad (3)$$

Where p is the solution accuracy larger the solution accuracy its better. Parameter Φ_{ext} is the extrapolated value of the infinitely larger number of mesh elements.it is possible to define a

characteristic equation with respect to the element size h. The size is proportional to the reciprocal value of the number of mesh elements (powered to 1/D).

$$h = \left(\frac{1}{N}\right)^{\frac{1}{D}} \quad h = \left(\frac{V}{N}\right)^{\frac{1}{D}}$$

Here, V is the volume of the cell. The dependency on the element size could be defined by the following equation

$$\Phi = \Phi_{\text{ext}} + a.h^p \quad (4)$$

Where the extrapolated value of the monitored quantity lies exactly at the vertical axis h = 0

In this case we could write three different equations for three different mesh elements size

$$\Phi = \Phi_{\text{ext}} + a.h_1^p \quad (5)$$

$$\Phi = \Phi_{\text{ext}} + a.h_2^p \quad (6)$$

$$\Phi = \Phi_{\text{ext}} + a.h_3^p \quad (7)$$

Subtracting the set of equations (2) from the set of equations (1) we can get

$$\Phi_1 - \Phi_2 = a.(h_1^p - h_2^p) = a.h_1^p \left(1 - \left(\frac{h_2}{h_1}\right)^p\right) = a.h_1^p \cdot (1 - r_{21}^p) \dots \dots \dots (8)$$

$$r_{21} = h_2/h_1$$

in a similar way we can write $r_{32} = h_3 / h_2$

$$\Phi_2 - \Phi_3 = a.h_2^p \cdot (1 - r_{32}^p) \quad (9)$$

dividing these two equations i.e (3) and (4)

$$\frac{\Phi_1 - \Phi_2}{\Phi_2 - \Phi_3} = \frac{1}{r_{21}^p} \cdot \left(\frac{1 - r_{21}^p}{1 - r_{32}^p}\right) \quad (10)$$

Separating power p and arranging we get an equation and adding logarithmic function we get

$$P = \frac{1}{\ln e_{21}^p} \cdot \left| \ln \left| \frac{\epsilon_{32}}{\epsilon_{21}} \right| + q \right|, \quad q = \ln \left(\frac{r_{21}^p - 8}{r_{32}^p - 8} \right), \quad s = \text{sign} \left(\frac{\epsilon_{32}}{\epsilon_{21}} \right)$$

$$a = \frac{\Phi_1 - \Phi_{ext}}{h_1^p}, \quad \Phi_{ext} = \frac{\Phi_1 r_{21}^p - \Phi_2}{r_{21}^p - 1}, \quad CGI_{21} = F_s \cdot \frac{\Phi_{ext} - \Phi_1}{\Phi_1}$$

F_s is the safety factor

$$CGI_{21} = \frac{1.25 \cdot e_a^{21}}{r_p^{21} - 1} \quad (11)$$

Where 1.25 represents the safety factor F_s in equal e_a^{21} is

$$e_a^{21} = \frac{\Phi_1 - \Phi_2}{\Phi_1} * 100\% \quad (12)$$

It is recommended to choose element sizes to get their ratio greater than 1.5

With reference to the entire chapter: I.B Celik, U.Ghia, P.J Roache, C.J Freitas, H.Coleman.,P.E Raad: Procedure for estimation and reporting of uncertainty due to discretization in CFD simulations, Journal of Fluid Engineering, 2008

The MATLAB script to represent the GRID CONVERGENCY INDEX

```
N = [ 147862 399396 900515 ];
Phi = [ 1.74e-3 7.26e-4 3.14e-3 ];% AVERAGE VELOCITY AT THE MEDIUM PLANE

[N, i] = sort(N,'descend'); % reverse order of elements so that the first element represent the
finest mesh
Phi = Phi(i);

figure(1);
plot(N,Phi,'r*', N,Phi,'b');
grid on;

D = 3; % dimension of the problem

r21 = (N(1)/N(2))^(1/D)
r32 = (N(2)/N(3))^(1/D)
if ( r21 < 1.3 || r32 < 1.3 )
    disp('refinement factors r21 and r32 should be greater than 1.3');
```

end

eps32 = Phi(3)-Phi(2)

eps21 = Phi(2)-Phi(1)

R = eps21/eps32

s = sign(eps32/eps21)

fq = @(p) log((r21.^p-s)./(r32.^p-s));

fp = @(p) p - 1/log(r21)*abs(log(abs(eps32/eps21))+fq(p));

%p = fzero(fp,1)

p = fsolve(fp,1)

Phi21ext = (r21^p*Phi(1)-Phi(2))/(r21^p-1)

e21a = abs((Phi(1)-Phi(2))/Phi(1))*100

CGI21 = 1.25*e21a/(r21^p-1)

e32a = abs((Phi(2)-Phi(3))/Phi(2))*100

CGI32 = 1.25*e32a/(r32^p-1)

CGI33 = 1.25*abs(Phi21ext-Phi(3))/Phi(3)*100

The following table represents the values that is calculated by running this MATLAB script

| quantity | Calculated value |
|----------|------------------|
| r21 | 1.313 |
| r32 | 1.3927 |
| eps32 | 0.0010 |
| eps21 | -0.0024 |
| R | -2.3807 |
| S | 1 |
| p | 3.8521 |
| Phi21ext | 0.0045 |
| e21a | 76.870 (%) |
| CGI21 | 52.2166 (%) |
| e32a | 139.6694 (%) |
| CGI32 | 67.6175 (%) |
| CGI33 | 194.8047 (%) |

Table 2: the calculated values by generating the MATLAB SCRIPT

Note: the refinement factors such as r21 and r32 must be greater than 1.3

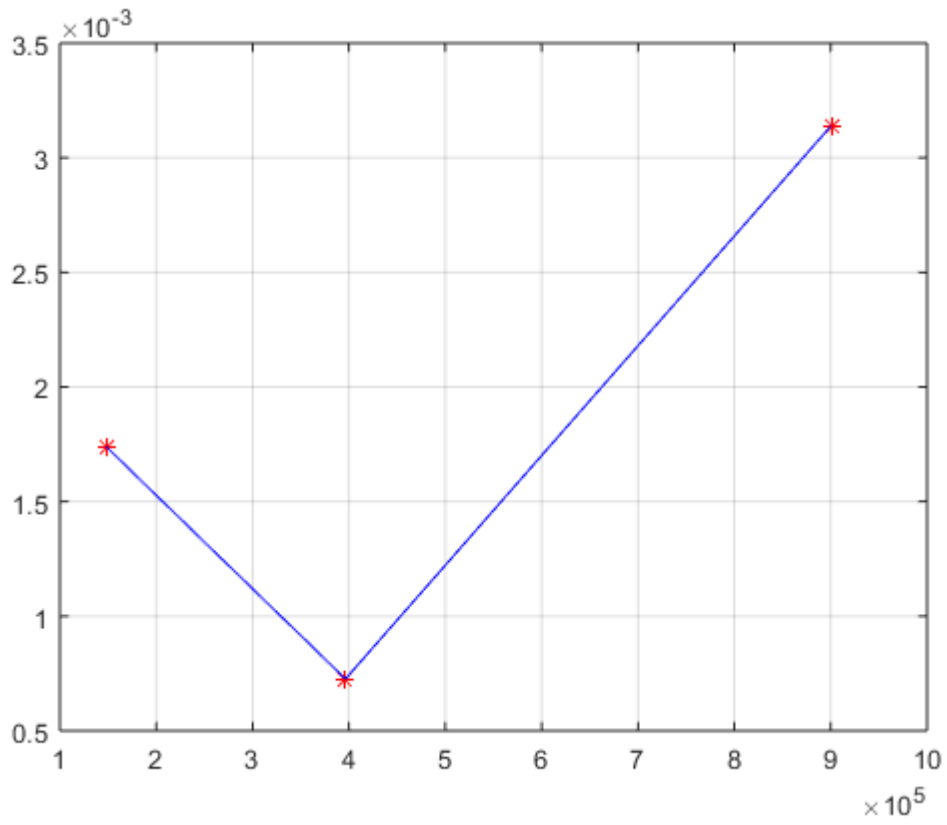


Figure 15: graph representing average velocity vs number of mesh (1-2-3 from left to right)

CHAPTER 5: INTRODUCTION TO CFD (COMPUTATIONAL FLUID DYNAMICS AND ITS METHODS) AND ITS WORKING TECHNIQUES

Computational fluid dynamics predicts the fluid flow, heat and mass transfer and chemical reactions by means of computer-based simulation.

To predict these phenomena the CFD uses equations based on the conservation of mass energy and momentum.

CFD can provide information on number of parameters such as

- Distribution of pressure, velocity, temperature
- Distribution of forces
- Distribution of phases (solid-liquid. Solid-gas)
- Species composition etc.

CFD used in all kinds of engineering processes

- Aerodynamics of aircraft and vehicles: lift and drag
- Hydrodynamics of ships
- Chemical process engineering such as mixing and separation. Polymer molding etc.
- Meteorology: weather prediction.
- Environmental engineering: distribution of pollutants and effluents.

From 1960s onwards, the aerospace industry has integrated CFD techniques into the design, manufacture of aircraft engines and jet engines. More recently the methods have been applied to the design of internal combustion engines, combustion chambers of gas turbines and furnaces. Furthermore, the motor vehicle manufacturers now predict drag forces under bonnet air flows and the in-car environment with the CFD.

The aim of the developments in the CFD field is to provide a capability with the other CAE (computer aided engineering) tools such as stress analysis codes.

There are several advantages of CFD over experiment-based approaches

- Major reduction in lead times and costs of new designs.
- Ability to study new systems where controlled experiments are difficult or impossible to perform.
- Very detailed report of results.

5.1: CFD WORK CODES (principles)

CFD codes are structured around the numerical algorithms that can tackle fluid flow problems.

Hence all codes are divided into three elements

- Preprocessor
- Solver
- Post processor

I would like to explain all the three elements briefly.

Preprocessor:

Preprocessor consists of the input flow of a problem so that it could be easily interpreted by the solver section of the CFD.

Preprocessor consists of several stages such as

- Definition of the geometry of the region of interest i.e. **computational domain**.
- Grid generation the subdivision of the domain into several smaller, non-overlapping domains such as grids, cells (or control volumes).
- Selection the physical and chemical phenomenon that needs to be modelled.
- Definition of fluid properties.
- Specification of approximate boundary conditions.

Solver:

There are three distinct streams of numerical solution techniques

- Finite element method
- Finite difference method
- Spectral methods.
- Finite volume method

We shall be primarily concerned with the finite volume method as the ANSYS FLUENT SOLVER depends on this method.

In outline the numerical algorithm consists of the following steps:

- Integration of the governing equations of fluid flow over all the control volumes of the domain.
- Discretization: conversion of the resulting integral equations into a system of the algebraic equations.
- Solution of the algebraic equations by an iterative method.

Post processing:

Post processing has several stages such as

- Domain geometry
- Vector plots
- Line and shaded contour plots
- 2D and 3D surface plots
- Particle tracking
- View manipulation
- Color port script

5.2: GOVERNING EQUATIONS AND ITS FORMS:

One of the major focuses of CFD is determining the flow behavior of the fluids or the fluid regime. Some of the equations are imperative in describing the viscous flow or the inviscid flow. These equations are determined from the Newton's laws of motions which also determines the stress in the fluid is the sum of the diffusing viscous term and the pressure term.

The continuity equation:

The continuity equation is defined as the transport of some quantity. It is simple when applying to some conserved quantity, but it can also be applied to series of extensive quantities such as mass, momentum and energy are conserved in some phenomenon. Hence it can be applied to number of physical quantities as well.

In differential form continuity equation can be written as

$$\frac{\partial \rho}{\partial t} + \nabla \cdot (\rho \vec{u}) = 0$$

Where \vec{u} is the flow velocity at a point and ρ is the density of the fluid. For incompressible flows the equation can be written as

$$\nabla \cdot \vec{u} = 0$$

Navier Stokes equation:

Navier Stokes equation is helpful in description of fluid flow also has number of practical uses in a wide range of engineering applications and physical applications.

The solution of the Navier Stokes equations is the flow velocity. The flow velocity is defined at a point or a region of space in simpler terms called a field. The velocity field is calculated once this field is evaluated the other terms pressure and temperature are determined automatically.

The general form of Navier Stokes equation is

$$\frac{D\vec{u}}{Dt} = -\nabla p + \nabla \cdot \vec{\tau} + \rho \vec{g}$$

∇p is the gradient of pressure

$\nabla \cdot \vec{\tau}$ is the divergence of dynamic stress tensor

$\rho \vec{g}$ is the volume forces (e.g. Gravity)

The Navier Stokes equation is a special form of Cauchy momentum equation. These are some of the governing equations in CFD analysis.

Solution of the governing equations:

With respect to the equations that are described above the numerical approach to the solution of these equations is not yet been developed. But the analytical approach can be described and evaluated by employing suitable discretization schemes by transformation of the parabolic equations into suitable algebraic equations or more precisely solvable algebraic equations. This is the crux of the numerical modeling in CFD (computational fluid dynamics).

A very general discretization scheme deployed in CFD analysis is *finite volume method* which is based upon dividing the computational domain in set of control volumes. The differential equations are integrated over the set of control volumes and divergence theorem is employed. To calculate the derivatives the values at the control volume faces are required which is based upon some assumption about its variation. The result of these equations is the set of algebraic equations one for each control volume which is solved iteratively.

CHAPTER 6: TURBULENCE AND ITS MODELS DESCRIPTION.

All flows encountered in engineering practices simple ones such as two-dimensional jets, wakes, pipes flow and flat plat boundary layers and more complicated three-dimensional ones become unstable above a certain Reynold's number. At low Reynolds number the flow is said to be laminar and at higher Reynold's number the flow is said to be turbulent.

A chaotic random state of motion develops in which the velocity and pressure change continuously with time within substantial regions of flow. (Versteeg and Malasekra,2015)

Flows in the laminar regime are completely described by the equations such as Navier Stokes and continuity equation. More complex flows can be solved numerically by CFD techniques such as the finite volume method without additional approximations.

First, we look at the main characteristics of turbulent flows. The Reynolds number of a flow gives a measure of the relative importance of inertia forces and viscous forces. In experiments on fluid systems. It is observed that at values below the so called the critical Reynolds number Re_{crit} the flow is smooth and adjacent layer of fluid slide past each other in an orderly fashion. If the applied boundary conditions do not change with time the flow is defined as **steady**. This regime is called **laminar flow**.

At values of the Reynolds number Re_{crit} a complicated series of events takes place which eventually leads to a radical change of the flow character.in the final state the flow behavior is random and chaotic. The motion becomes intrinsically unsteady even with constant imposed boundary conditions. The velocity and all other properties vary in a random and chaotic way. This regime is called **turbulent flow**.

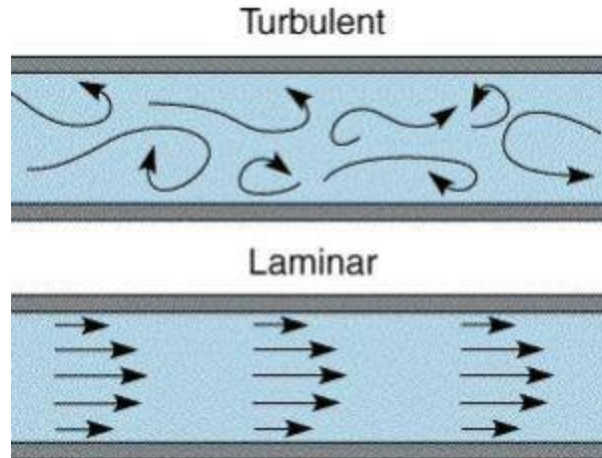


Figure 16: A typical representation of the turbulent flow and laminar flow (Esfscience,2012)

6.1: TURBULENCE FLOW CALCULATIONS:

Turbulence causes the appearance in the flow of eddies with a wide variety of length and time scales that interact in a dynamically complex way. Given the importance of the avoidance or promotion of turbulence in engineering applications, it's no surprise that the substantial amount of research is dedicated to the development of numerical methods to capture the important effects due to turbulence.

Turbulence models for Reynolds averaged Navier Stokes equations (RANS):

This attention is focused on the mean flow and the effects of turbulence on mean flow properties. Prior to the application of numerical methods, the Navier Stokes equations are time averaged. Extra terms appear in the time averaged equations due to the fluctuations between turbulence models. Owing to these extra terms we solve classical turbulence models like k-epsilon and the Reynold stress model.

Large eddy simulation (LES):

This is an intermediate form of turbulence calculations which tracks the behavior of the larger eddies. The method involves space filtering of the unsteady Navier Stokes equations prior to the computations. Which passes the larger eddies and smaller eddies.

Direct numerical simulation (DNS):

These simulations compute the mean flow and all turbulent velocity fluctuations. The unsteady Navier Stokes equations are solved on spatial grids that are sufficiently fine that they can resolve the Kolmogorov length scales at which energy dissipation takes place and with time steps sufficiently small to resolve the period of fastest fluctuations.

RANS Turbulence models

Turbulence are the result of fluctuated velocity fields. Because of these fluctuated velocity fields there is a lot of oscillation in the various transport properties such as momentum energy and concentration etc. to calculate these fluctuations and simulate will be expensive due to these fluctuations will be in small scales and high frequencies. As a result of this problem we evaluate time averaged or ensembled averaged equations so that we could considerably reduce computational expenses minimize small scales and perform simulations.

There are various types of turbulence models like

- Spallart Almaras
- K-epsilon
- K-omega
- RSM

Spallart Almaras:

Economical for larger meshes. Good for mildly complex (quasi 2-D), external/internal flows and boundary layer flows under pressure gradients (e.g. airfoils, wings, airplanes).

k-epsilon:

k-epsilon is a standard two equation turbulence model which has a lot of various types such as

- Standard k-epsilon
- Realizable k-epsilon
- RNG k-epsilon

We will discuss about the above-mentioned turbulence models one by one.

Standard k-epsilon: robust widely used despite known limitations of the model. Perform poorly complex flows involving severe pressure gradient separation.

Realizable k-epsilon: suitable for complex flows involving rapid strain. Moderate swirl and vortices.

RNG (renormalization group) k- epsilon: offers largely the same benefits and has similar application as realizable.

k-omega:

It's also again two transport equation model also most widely and takes a little more time for the computational time when compared to the k-epsilon.

There are also various types of k-omega models such as

- Standard k-omega
- SST k-omega

Standard k-omega: superior performance wall bounded layers free shear and low Re compare to the k-epsilon family. Suitable for complex boundary and overpressure gradient.

SST (shear stress transport) k-omega: offers similar benefits as standard k-omega. Not overly sensitive to inlet boundary conditions like the standard k-omega.

Mean and instantaneous velocities:

As discussed about the various turbulence models one of the primary points to discuss about the turbulence is the calculation of the mean and instantaneous velocities.

The instantaneous velocity(U) would look like this

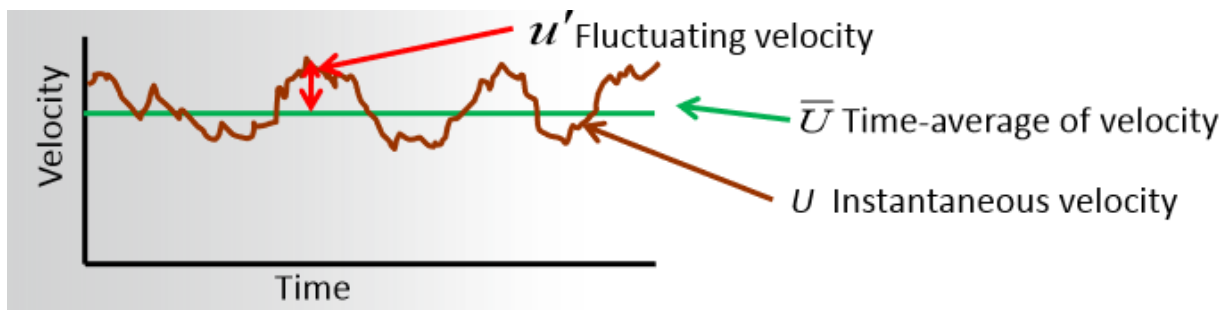


Figure 17 : representation of instantaneous velocity and time average velocity (ANSYS TRAINING MATERIALS,2018)

At any point of time the velocity $U = \bar{U} + u'$

Where u' is the fluctuating velocity and \bar{U} is the time averaged velocity as described in the above Figure.17

Turbulent viscosity:

The turbulent viscosity is defined by the equation as shown below

$$\mu_t = \rho C_\mu \frac{k^2}{\varepsilon}$$

μ_t is the turbulent viscosity (m^2/s)

ρ is the density of the fluid (kg/m^3)

C_μ is an empirical constant

K is the turbulent kinetic energy (m^2/s^2)

ε is the kinetic energy dissipation rate (m^2/s^3)

Estimation of the Y plus value for conical fish tank:

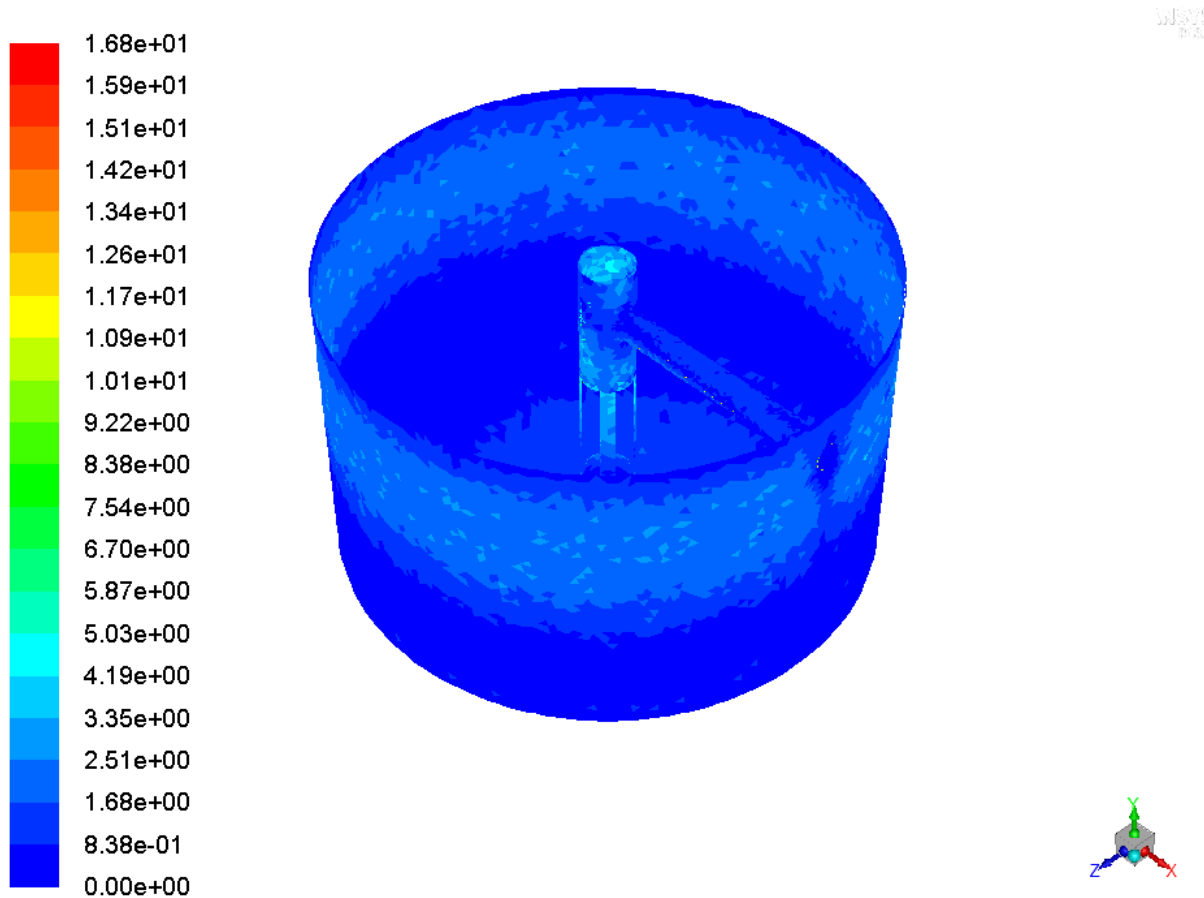


Figure 18: Illustration of the tank for the y plus

The Y plus can be generated in the case of conical fish tank design can be generated using the results → display → surface integrals.

Under the dropdown menu for turbulence we generate Y plus value which in the case of conical fish tank design is 2.66 the criterion for the Y plus value is recommended to be around 1. The enhanced wall treatment setting in Fluent solver enables using wall functions in case this condition is not met. In such case, the velocity profiles near walls are only approximative.

Enhanced wall Treatment:

Standard k- epsilon model is not capable enough to simulate the flow in the vicinity of the wall. This inconsistency is resolved by the introduction of the 2-layer model. The computational domain is bifurcated into two regions; viscosity near the wall and fully turbulent region. The separation between the two regions is defined in terms of distance of the wall.

Enhanced wall treatment is near modeling method that combines a 2-layer model with so called enhanced wall functions, If the near wall mesh is fine enough to be able to resolve the viscous sublayer, then the enhanced wall treatment will be identical to the traditional 2- layer model.

However, the restriction that the near wall mesh must be sufficiently fine everywhere demands a large computational requirement.

To achieve the goal of having a near wall modeling approach that will have the accuracy of standard 2-layer approach for finer near wall mesh and at the same time will not substantially reduce the accuracy for wall function meshes. ANSYS Fluent combines the 2-layer model with enhanced wall functions.

CHAPTER 7: RESULTS AND DISCUSSION

7.1: CFD MODEL TO PROBLEM SOLUTION

As described in the “objectives and motivation of the work “to study the hydrodynamics of the fish tanks to determine the flow rates and the velocity profiles for the breeding of fishes in the fish tanks. A CFD model can be proposed for the study and using ANSYS Fluent solver. Computational fluid dynamics allows to perform several simulations by breaking the computational domain into the set of algebraic equations.

The accuracy of the solution depends upon number of factors such the number of mesh elements, the complexity of the model and defining precise boundary conditions for the problem solution. Though higher the number of mesh elements the accuracy of the solution gets better at the cost of computational power.

Solution procedure:

CFD simulations were performed on the discretized model of the fish tank using ANSYS Fluent solver and calculation of the velocities at different points in the fish tank were done and compared with the experimental results (journal of fish biology.2015, Crete, Greece).

Setting up the fluent solver:

Setting up the fluent solver involves several steps such as models, materials and cell zone conditions and boundary conditions. Here some of brief description of the various parameters that was mentioned and the values that was used

Models:

There can be several models that can used in ANSYS Fluent such as discrete phase models, viscous models, multiphase models etc.

Here viscous model is deployed which bifurcates into parts that are laminar and turbulence models. In this setting of the fluent solver three turbulence models are employed for better representation and comparison.

Materials:

Material for the conical tank

Fluid – water with density ($\rho = 1000 \text{ kg/m}^3$)

Solid – aluminum

Models:

Viscous – standard (k- epsilon)

Cell zone conditions:

Fluid

Boundary conditions:

Inlet velocity – different inlet velocities are used (0.05 m/s and 0.07 m/s)

Interior – solid(interior)

Outlet – pressure (outlet)

Surface – symmetry

Wall – solid (stationary)

Initialization:

Hybrid initialization was employed.

Below are some of the results for the respective numerical model with discussion and some comparisons.

For the calculation of the inlet velocity for the fish tank the volumetric flow rate of the tank was given as per the experimental data (K Lika et al ,2015). In a 500-liter tank the water was provided from the bottom of the fish tank and regulated at different volumetric flow rates

approximately 75 to 100 percent of the volume (per hour). So, the calculation would be done according to the given volumetric flow rate.

Hence, for a 500-liter tank considering 100% of the total volume the water is circulated per hour would give us

Volumetric flow rate as $\dot{V} = 500$ liter/ per hour

Converting volumetric flow rate liters/hour to m^3/sec would give $\dot{V} = 1.388 \times 10^{-4} \text{ m}^3/\text{sec}$

Calculating velocity through the inlet pipe from the volumetric flow rate

$\dot{V} = \text{area of the cross-section pipe} * \text{velocity through the pipe}$

$$1.388 \times 10^{-4} = \pi r^2 * u \quad [6.1]$$

Where u is the velocity through the pipe or precisely inlet velocity through the pipe.

r is the radius of the pipe (m)

$$1.388 \times 10^{-4} = \pi * (.025)^2 * u$$

Where $u = 0.07 \text{ m/sec}$ is the calculated inlet velocity

Henceforth we can calculate Reynolds number from the formula for turbulence check

$Re = \frac{ud}{\nu}$ where d is the diameter of the pipe(m) and u is the velocity of the water through inlet (m^2/s) and ν is the kinematic viscosity of water (m^2/s)

Kinematic viscosity of water at 20°C is $\nu = 1.0035 \times 10^{-6} \text{ m}^2/\text{sec}$ (*engineering toolbox.com, 2015*)

$$\text{Calculating Reynolds number } Re = \frac{0.07*(0.05)}{1.0035*10^{-6}} = 3487.79$$

which is greater than the required limit of the flow through the circular pipe condition for Reynolds number ($Re > 2300$) that means turbulence model is proposed for the calculation. With respect to the above settings that was set in fluent solver.

The iterations were performed in several turbulence models. The residuals of various turbulence models are illustrated in the subsequent pages and the comparison with the experimental data was done was also analyzed.

Convergence criteria:

One of the important considerations in ANSYS fluent is the representation of the scaled residuals after performing the iterations the convergence criteria for the residuals usually is in the order

10^{-3} and may be below 10^{-4} (afs.enea.it, ANSYS, 2015). Except in some cases the criterion may be in the order of 10^{-6} .

7.2: RESULTS AND COMPARISON

The simulation results have been examined in K-epsilon and K-omega model. As mentioned, the results have been compared with experimental data.

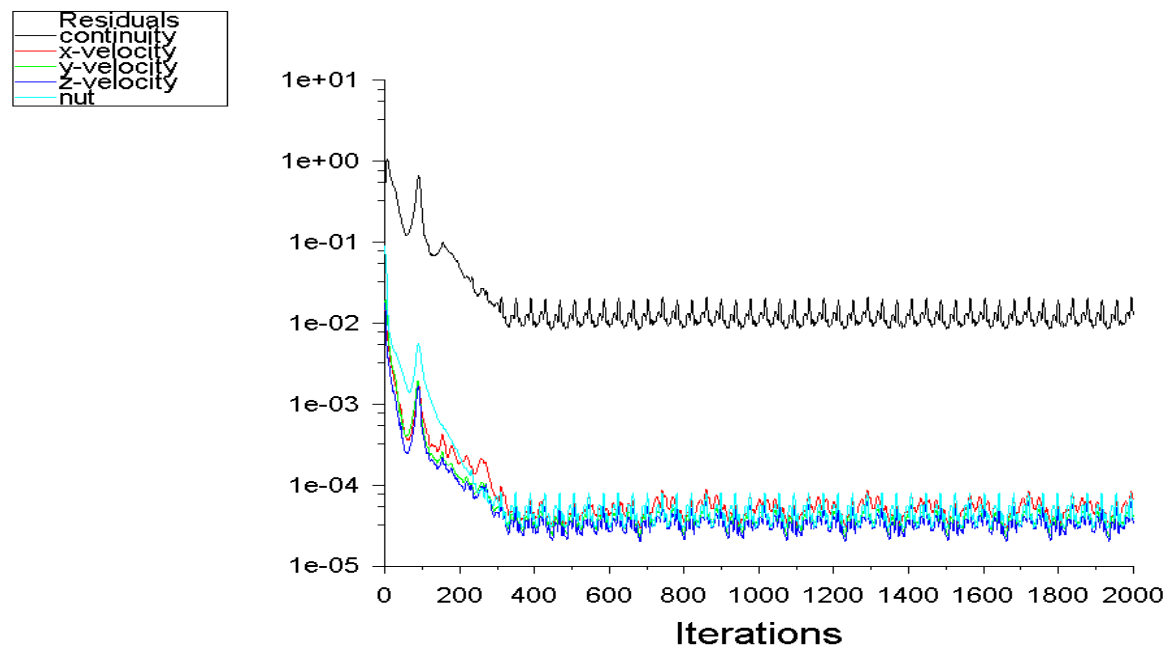


Figure 19: representation of Spallart Almaras model

Spallart Almaras model has been considered as the first stage of the simulation results because it's the least time consuming and a simple proposed model for the simulation calculation.

(In the previous work Mr. Jaroslav Hanak provided relatively good results with coarser meshes)

Some of the results that has been obtained from the calculation of the velocities at different points on a plane in fish tanks.

One of the important considerations that we took before simulating the velocities at different coordinates for calculation.

First, the points are created around the medium plane for calculating the velocities at those points.

The option that's used is **Create → point**

With reference to the experimental data the x, y, z coordinated points are mentioned in Table 1

$$x = -0.45, y = 0, z = .25$$

With reference to the experimental data obtained from the journal obtained coordinates that was used in the ANSYS Fluent

$$-y = x, -z = y, -x = z$$

Referring to the above example

$$0 = x, -0.25 = y, 0.45 = z$$

This is the method how we simulated the values in ANSYS fluent

Note: all the tabular data displayed here are in terms of velocity (m/s)

| x(m) | y(m) | z(m) | Experimental data(m/s) | Simulated data(m/s) |
|-------|-------|-------|------------------------|----------------------|
| 0 | -0.25 | 0.45 | $2.25 \cdot 10^{-3}$ | $1.4 \cdot 10^{-3}$ |
| 0.45 | -0.25 | 0 | $9.47 \cdot 10^{-3}$ | $1.7 \cdot 10^{-3}$ |
| 0 | -0.25 | -0.45 | $5.84 \cdot 10^{-3}$ | $1.3 \cdot 10^{-3}$ |
| -0.45 | -0.25 | 0 | $6.46 \cdot 10^{-3}$ | $3.1 \cdot 10^{-3}$ |
| 0 | -0.30 | 0.25 | $2.07 \cdot 10^{-3}$ | $1.39 \cdot 10^{-3}$ |
| 0.25 | -0.30 | 0 | $5.24 \cdot 10^{-3}$ | $1.30 \cdot 10^{-3}$ |
| 0 | -0.30 | 0.10 | $5.60 \cdot 10^{-3}$ | $1.9 \cdot 10^{-3}$ |
| 0.10 | -0.30 | 0 | $2.17 \cdot 10^{-3}$ | $1.9 \cdot 10^{-3}$ |
| -0.10 | -0.30 | 0 | $6.05 \cdot 10^{-3}$ | $1.8 \cdot 10^{-3}$ |
| -0.25 | -0.30 | 0 | $9.12 \cdot 10^{-3}$ | $1.63 \cdot 10^{-3}$ |

Table 3: experimental vs simulated (Spallart Almaras)

k-epsilon model:

With an inlet velocity of 0.05 m/s was employed in ANSYS fluent and some simulations were performed in the ANSYS Fluent.

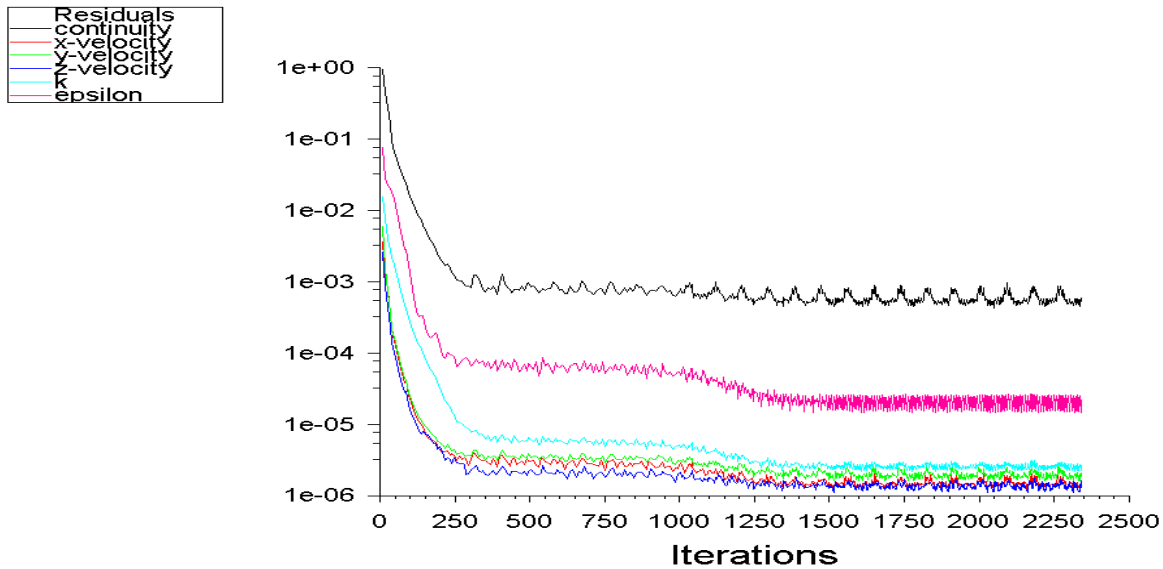


Figure 20: representation of k epsilon model

| x(m) | y(m) | z(m) | Experimental data(m/s) | Simulated data(m/s) |
|-------|-------|-------|------------------------|---------------------|
| 0 | -0.25 | 0.45 | $2.25 * 10^{-3}$ | $2.01 * 10^{-3}$ |
| 0.45 | -0.25 | 0 | $9.47 * 10^{-3}$ | $1.9 * 10^{-3}$ |
| 0 | -0.25 | -0.45 | $5.84 * 10^{-3}$ | $2.1 * 10^{-3}$ |
| -0.45 | -0.25 | 0 | $6.46 * 10^{-3}$ | $2.06 * 10^{-3}$ |
| 0 | -0.30 | 0.25 | $2.07 * 10^{-3}$ | $1.13 * 10^{-3}$ |
| 0.25 | -0.30 | 0 | $5.24 * 10^{-3}$ | $1.0 * 10^{-3}$ |
| 0 | -0.30 | 0.10 | $5.60 * 10^{-3}$ | $5.2 * 10^{-3}$ |
| 0.10 | -0.30 | 0 | $2.17 * 10^{-3}$ | $5.18 * 10^{-3}$ |
| -0.10 | -0.30 | 0 | $6.05 * 10^{-3}$ | $4.7 * 10^{-3}$ |
| -0.25 | -0.30 | 0 | $9.12 * 10^{-3}$ | $5.03 * 10^{-3}$ |

Table 4: experimental vs simulated (k-epsilon realizable)

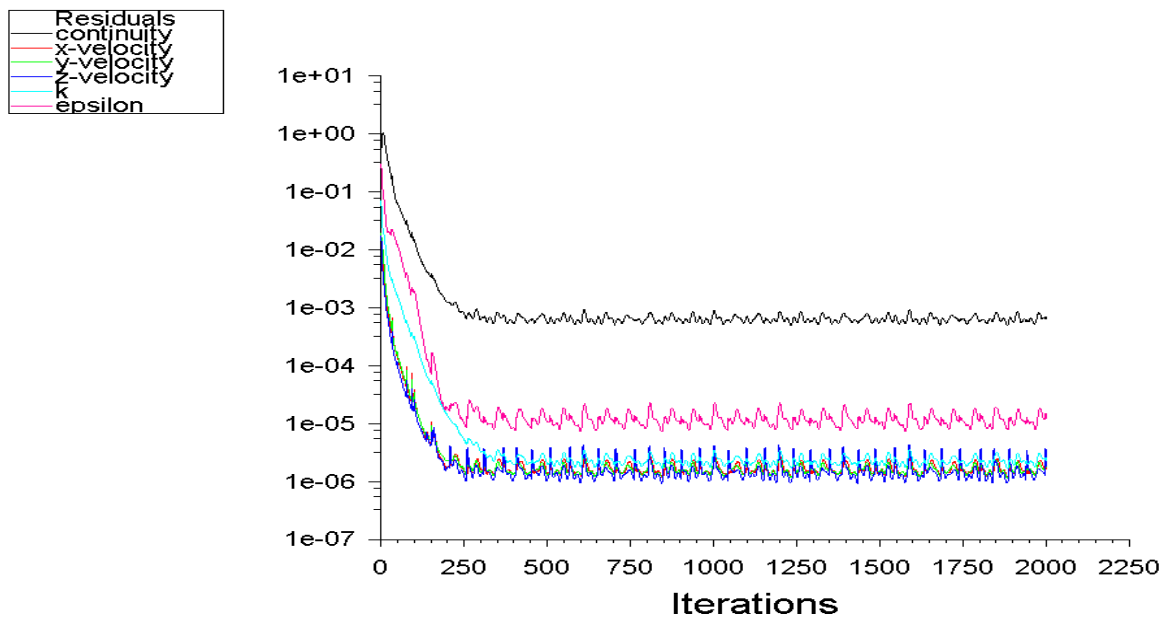


Figure 21: representation of k-epsilon model(realizable)

| x(m) | y(m) | z(m) | Experimental data(m/s) | Simulated data(m/s) |
|-------|-------|-------|------------------------|---------------------|
| 0 | -0.25 | 0.45 | $2.25 * 10^{-3}$ | $2.49 * 10^{-3}$ |
| 0.45 | -0.25 | 0 | $9.47 * 10^{-3}$ | $2.31 * 10^{-3}$ |
| 0 | -0.25 | -0.45 | $5.84 * 10^{-3}$ | $2.75 * 10^{-3}$ |
| -0.45 | -0.25 | 0 | $6.46 * 10^{-3}$ | $2.51 * 10^{-3}$ |
| 0 | -0.30 | 0.25 | $2.07 * 10^{-3}$ | $1.2 * 10^{-3}$ |
| 0.25 | -0.30 | 0 | $5.24 * 10^{-3}$ | $1.5 * 10^{-3}$ |
| 0 | -0.30 | 0.10 | $5.60 * 10^{-3}$ | $6.5 * 10^{-3}$ |
| 0.10 | -0.30 | 0 | $2.17 * 10^{-3}$ | $6.0 * 10^{-3}$ |
| -0.10 | -0.30 | 0 | $6.05 * 10^{-3}$ | $7 * 10^{-3}$ |
| -0.25 | -0.30 | 0 | $9.12 * 10^{-3}$ | $8.5 * 10^{-3}$ |

Table 5: experimental vs simulated (k-epsilon realizable)

Here we can assess that there are certain changes not drastically, but the results have quite improved but still there are some errors some of the velocity calculations that goes along with the experimental data. These simulations were performed with an increased number of mesh elements (397,396 elements).

For much better comparison the results have been compared with little higher number of mesh elements (900515 elements) as illustrated in the figure below.

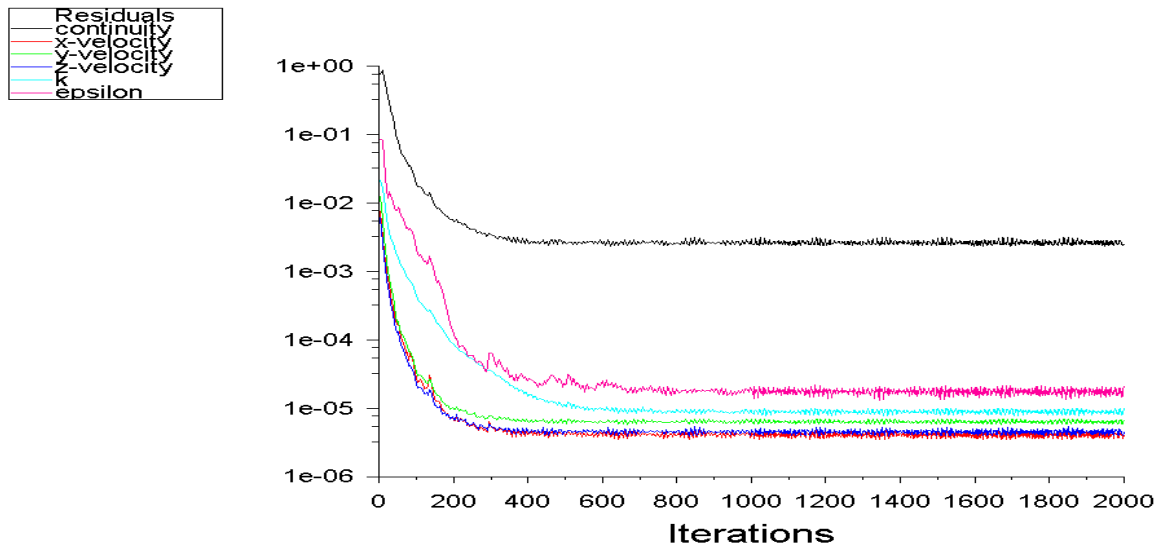


Figure 22: representation of k-epsilon(realizable)

| x(m) | y(m) | z(m) | Experimental data(m/s) | Simulated data(m/s) |
|-------|-------|-------|------------------------|---------------------|
| 0 | -0.25 | 0.45 | $2.25 * 10^{-3}$ | $2.5 * 10^{-3}$ |
| 0.45 | -0.25 | 0 | $9.47 * 10^{-3}$ | $2.2 * 10^{-3}$ |
| 0 | -0.25 | -0.45 | $5.84 * 10^{-3}$ | $2.4 * 10^{-3}$ |
| -0.45 | -0.25 | 0 | $6.46 * 10^{-3}$ | $2.1 * 10^{-3}$ |
| 0 | -0.30 | 0.25 | $2.07 * 10^{-3}$ | $1.1 * 10^{-3}$ |
| 0.25 | -0.30 | 0 | $5.24 * 10^{-3}$ | $2.4 * 10^{-3}$ |
| 0 | -0.30 | 0.10 | $5.60 * 10^{-3}$ | $5.90 * 10^{-3}$ |
| 0.10 | -0.30 | 0 | $2.17 * 10^{-3}$ | $5.2 * 10^{-3}$ |
| -0.10 | -0.30 | 0 | $6.05 * 10^{-3}$ | $4.7 * 10^{-3}$ |
| -0.25 | -0.30 | 0 | $9.12 * 10^{-3}$ | $8.012 * 10^{-3}$ |

Table 6: experimental vs simulated (k-epsilon realizable)

k-omega model (SHEAR STRESS TRANSPORT)

With the same inlet velocity as above (0.05 m/s) and with the same number of mesh elements (900,000 elements). The iterative calculation is shown in the figure below.

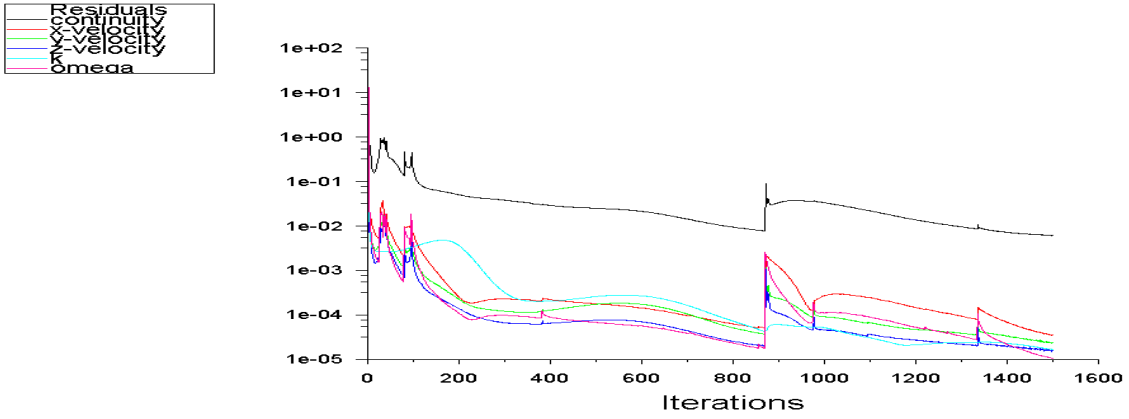


Figure 23: representation of the k-omega (SST)

| x(m) | y(m) | z(m) | Experimental data(m/s) | Simulated data(m/s) |
|-------|-------|-------|------------------------|-----------------------|
| 0 | -0.25 | 0.45 | $2.25 \cdot 10^{-3}$ | $2.80 \cdot 10^{-3}$ |
| 0.45 | -0.25 | 0 | $9.47 \cdot 10^{-3}$ | $5.2 \cdot 10^{-3}$ |
| 0 | -0.25 | -0.45 | $5.84 \cdot 10^{-3}$ | $7.7 \cdot 10^{-3}$ |
| -0.45 | -0.25 | 0 | $6.46 \cdot 10^{-3}$ | $6.7 \cdot 10^{-3}$ |
| 0 | -0.30 | 0.25 | $2.07 \cdot 10^{-3}$ | $1.7 \cdot 10^{-3}$ |
| 0.25 | -0.30 | 0 | $5.24 \cdot 10^{-3}$ | $1.72 \cdot 10^{-3}$ |
| 0 | -0.30 | 0.10 | $5.60 \cdot 10^{-3}$ | $1.780 \cdot 10^{-3}$ |
| 0.10 | -0.30 | 0 | $2.17 \cdot 10^{-3}$ | $1.9 \cdot 10^{-3}$ |
| -0.10 | -0.30 | 0 | $6.05 \cdot 10^{-3}$ | $1.8 \cdot 10^{-3}$ |
| -0.25 | -0.30 | 0 | $9.12 \cdot 10^{-3}$ | $1.25 \cdot 10^{-3}$ |

Table 7: representation of the k-omega model (SST)

We have also compared the results with k-omega (SST) with the higher number of mesh elements such as (900,000) and with the inlet velocity (0.07 m/s)

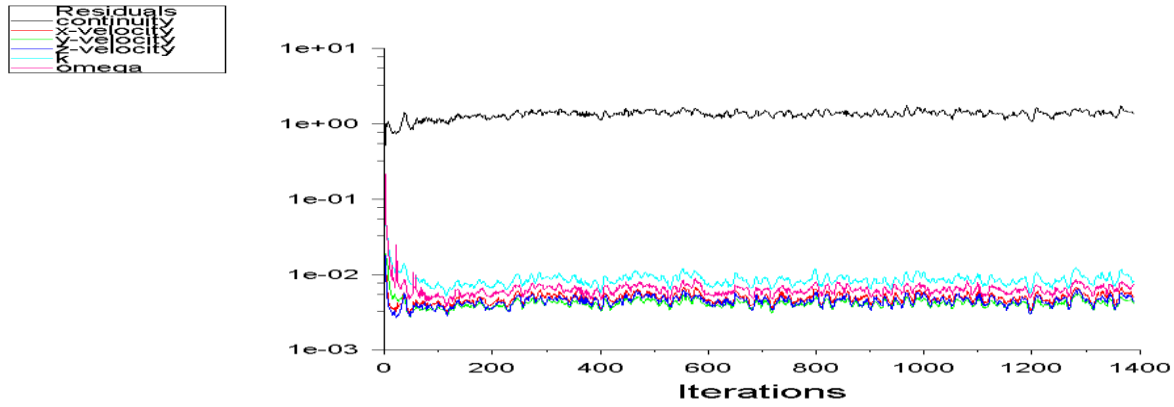


Figure 24: representation of the k-omega SST

The figure shown above is not a recommended model for the data comparison because the solution hasn't reached a convergence. But we have still tried to compare the results with the experimental data. The table is shown below.

| x(m) | y(m) | z(m) | Experimental data(m/s) | Simulated data(m/s) |
|-------|-------|-------|------------------------|---------------------|
| 0 | -0.25 | 0.45 | $2.25 * 10^{-3}$ | 0.00037 |
| 0.45 | -0.25 | 0 | $9.47 * 10^{-3}$ | $2.5 * 10^{-3}$ |
| 0 | -0.25 | -0.45 | $5.84 * 10^{-3}$ | $2.2 * 10^{-3}$ |
| -0.45 | -0.25 | 0 | $6.46 * 10^{-3}$ | $3.3 * 10^{-3}$ |
| 0 | -0.30 | 0.25 | $2.07 * 10^{-3}$ | $2.04 * 10^{-3}$ |
| 0.25 | -0.30 | 0 | $5.24 * 10^{-3}$ | $3.6 * 10^{-3}$ |
| 0 | -0.30 | 0.10 | $5.60 * 10^{-3}$ | $2.877 * 10^{-3}$ |
| 0.10 | -0.30 | 0 | $2.17 * 10^{-3}$ | $3.07 * 10^{-3}$ |
| -0.10 | -0.30 | 0 | $6.05 * 10^{-3}$ | $2.562 * 10^{-3}$ |
| -0.25 | -0.30 | 0 | $9.12 * 10^{-3}$ | $3.25 * 10^{-3}$ |

Table 8: experimental vs simulated (k-omega SST)

k-epsilon model:

By employing K epsilon model for lower inlet velocity (0.035 m/s) with standard wall functions with the mesh elements of (397,296 elements). The experimental data vs simulated can be displayed in the results though it reached convergence limit but still the solution hasn't converged as expected.

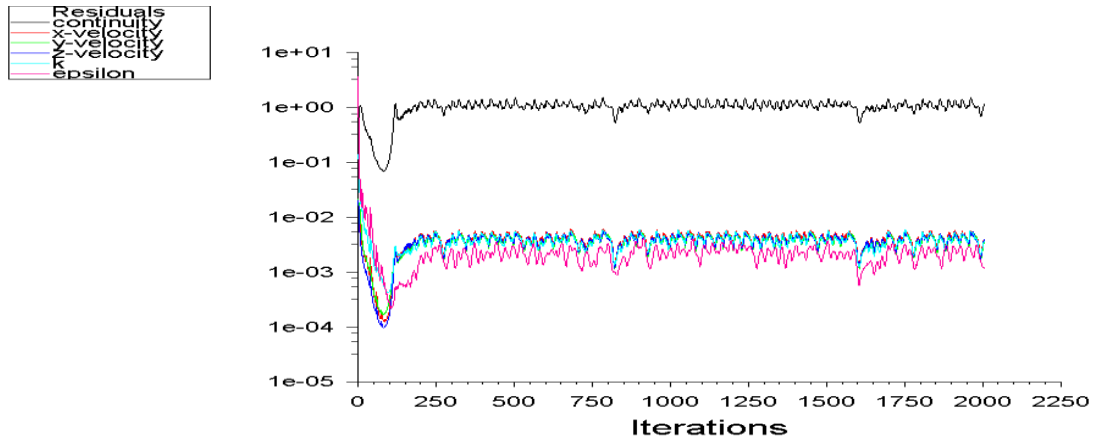


Figure 25: representation of the k epsilon standard wall

| x(m) | y(m) | z(m) | Experimental data(m/s) | Simulated data(m/s) |
|-------|-------|-------|------------------------|---------------------|
| 0 | -0.25 | 0.45 | $2.25 \cdot 10^{-3}$ | 0.00024601 |
| 0.45 | -0.25 | 0 | $9.47 \cdot 10^{-3}$ | 0.00082890 |
| 0 | -0.25 | -0.45 | $5.84 \cdot 10^{-3}$ | 0.00021927 |
| -0.45 | -0.25 | 0 | $6.46 \cdot 10^{-3}$ | 0.00055698 |
| 0 | -0.30 | 0.25 | $2.07 \cdot 10^{-3}$ | 0.00075253 |
| 0.25 | -0.30 | 0 | $5.24 \cdot 10^{-3}$ | 0.00080029 |
| 0 | -0.30 | 0.10 | $5.60 \cdot 10^{-3}$ | 0.00098315 |
| 0.10 | -0.30 | 0 | $2.17 \cdot 10^{-3}$ | $1.2 \cdot 10^{-3}$ |
| -0.10 | -0.30 | 0 | $6.05 \cdot 10^{-3}$ | $1.2 \cdot 10^{-3}$ |
| -0.25 | -0.30 | 0 | $9.12 \cdot 10^{-3}$ | $1.4 \cdot 10^{-3}$ |

Table 9: experimental vs simulated (k-epsilon realizable)

The average velocities of the various planes are calculated and has been compared to the velocities experimentally (K Lika et al, journal of fish biology, 2015).

| Planes | Simulated data (m/s) | Experimental data (m/s) | % change |
|--------------|--------------------------|---|----------|
| Plane medium | 7.80541×10^{-4} | $7.18 \times 10^{-3} \pm 1.12 \times 10^{-3}$ | 89 |
| Bottom | 1.688×10^{-3} | $8.27 \times 10^{-3} \pm 1.12 \times 10^{-3}$ | 50 |
| Surface | 1.38923×10^{-3} | $1.11 \times 10^{-2} \pm 1.19 \times 10^{-2}$ | 88 |
| Average | 1.2858×10^{-3} | $5.77 \times 10^{-3} \pm 3.43 \times 10^{-3}$ | 62 |

Table 10: The average velocities are calculated for the mesh elements (173,882).

| Planes | Simulated data (m/s) | Experimental data (m/s) | %change |
|--------------|-------------------------|---|---------|
| Plane medium | 2.2×10^{-3} | $7.18 \times 10^{-3} \pm 1.12 \times 10^{-3}$ | 96 |
| Bottom | 1.7×10^{-3} | $8.27 \times 10^{-3} \pm 1.12 \times 10^{-3}$ | 51 |
| Surface | 4.75×10^{-3} | $1.11 \times 10^{-2} \pm 1.19 \times 10^{-2}$ | 60 |
| Average | 2.833×10^{-3} | $5.77 \times 10^{-3} \pm 3.43 \times 10^{-3}$ | 17 |

Table 11: The average velocities are calculated for the mesh elements (397,396)

| Planes | Simulated data (m/s) | Experimental data (m/s) | %change |
|--------------|-------------------------|---|---------|
| Plane medium | 2.09×10^{-3} | $7.18 \times 10^{-3} \pm 1.12 \times 10^{-3}$ | 86 |
| Bottom | 1.71×10^{-3} | $8.27 \times 10^{-3} \pm 1.12 \times 10^{-3}$ | 52 |
| Surface | 4.45×10^{-3} | $1.11 \times 10^{-2} \pm 1.19 \times 10^{-2}$ | 62 |
| Average | 2.75×10^{-3} | $5.77 \times 10^{-3} \pm 3.43 \times 10^{-3}$ | 19 |

Table 12: The average velocities are calculated for the mesh elements (900,515)

According to the above tables we can assess that the results seems to be good.

The average velocities over the entire plane for the fish tank design is calculated with respect to the number of mesh elements over the plane in ANSYS Fluent.

7.3: DISCRETE PHASE MODELS

When we discuss about discrete phase models, we always try to assess the multiphase flows in CFD models or in a computational domain.

Multi-phase flows are supplying fluid flow system consisting of two or more distinct phases flowing simultaneously in mixture. Multi-phase flow exists in many different forms such two phase flows

- Gas – liquid
- Gas – solid mixture
- Liquid -solid
- Immiscible liquid mixture

Gas-solid flow: identified as gas -solid or gas droplet flows is concerned with motion of the suspended solid or gas droplet in gas phase.

Depending upon the particle number density these flows can be either dilute or dense.

Liquid- solid: consisting of solid particles in liquid flow. Also referred as slurry transportation. Which is mostly applied in food or mineral processing industry.

Gas-liquid: gas liquid flow can assume several configurations such as

- Dispersed flows
- Mixed or transitional flows
- Separated flows

Examples of dispersed flow are motion of bubbles in liquid and liquid droplets in gas.

There are some fundamental definitions relating discrete phase flows

Superficial velocity:

$$u_q = \frac{\dot{M}}{\rho_q A}$$

Superficial velocity of the phase is described by mass flow rate (\dot{M}) [kg/s] of the phase divided by the density of the phase(ρ) multiplied by the area of the pipe(A) [m²]

Phase velocity: its defined by the superficial velocity divided by the volume fraction

$$v_q = \frac{u_q}{\alpha_q}$$

v_q is the phase velocity (m/s)

α_q is the volume fraction

Stokes number: it gives the temporal correlation between particle velocity and the fluid velocity

$$S_t = \frac{\tau_p}{\tau_q}$$

τ_p is the particle velocity (m/s) and the τ_q is the fluid velocity (m/s)

$S_t \ll 1$ the particle response time is much less than the characteristic associated with the flow field. In this case the particles will have ample time to respond to changes in flow velocity and particle and fluid particles will be nearly equal.

$S_t \gg 1$ then the particles will have essentially no time respond to the fluid velocity changes and the particle velocity will be little affected by fluid velocity change.

7.3.1: RESIDENCE TIME DISTRIBUTION

The discrete phase model has been established in the case of conical fish tank and the residence time distribution analysis has been made and compared with the circular tank geometries and rectangular tank geometries.

The residence time distribution measurement and flow patterns are the crux of establishing hydrodynamics of the fish tanks.

The hydrodynamics of the fish tanks is the most important in terms of fish welfare due to avoidance of recirculating and low velocity zones (Pascal Klebert,2018). The self-cleaning of the fish tanks expressed as a removal of the intact solid waste minimizes the mechanical breakdown of the particles and reduces the cost of subsequently separating the solid waste from a single effluent stream (Davidson and Summerfelt, 2005).

The major objective to study the residence time distribution to ensure proper water mixing for the tanks because poor water mixing conditions can influence the welfare of the fish in a tank in physiology (Odeh et al., 2003) fish exercise and behavior (Ross and Wattern, 1998) and aggression and social hierarchies (Griffith and Armstrong , 2000).

The analyzing of the particles or fish food pellets is introduced in the conical tank and the residence time has been analyzed in the cases of conical fish tank, circular tank and rectangular tank geometries. Of all these geometries experimental was not available and the comparison has been made for better representation and future works at least in the case of conical fish tank geometries.

Solution procedure:

Firstly, the iterations must be performed to reach convergence limit

Models – discrete phase

In the submenu of discrete phase

- creation of injections is required
- specifying diameter of the fish feed pellets for e.g. 0.001 m or 0.005m
- flow rate – 0.005 kg/s or 0.05 kg/s
- y velocity – 9.81 m/s
- injection type – surface
- release from – surfaces (for all tank geometries)

particle type: Inert

Materials: Here the density can be specified (for e.g. 1800 kg/m³ or 2000 kg/ m³)

Post processing section:

Under the section of particle tracking we can specify the particles residence time and under the options tick mark the **node values** and **auto range**.

Comparison of residence time

Conical tank design

| Diameter(mm) | density of the particle (kg/m ³) | Flow rate (kg/s) | Residence time (seconds) |
|--------------|--|------------------|--------------------------|
| 1mm | 2000 | 0.005 | 2705 |
| 1mm | 1800 | 0.05 | 17130 |
| 5mm | 2000 | 0.005 | 294.5 |
| 5mm | 1800 | 0.05 | 15130 |

Table 13: residence time distribution of conical tank

Circular tank design

| Diameter(mm) | density of the particle (kg/m ³) | Flow rate (kg/s) | Residence time (seconds) |
|--------------|--|------------------|--------------------------|
| 1mm | 2000 | 0.005 | 11.22 |
| 1mm | 1800 | 0.05 | 11.23 |
| 5mm | 2000 | 0.005 | 3.3 |
| 5mm | 1800 | 0.05 | 3.4 |

Table 14: residence time distribution of the circular tank

Rectangular tank design

| Diameter(mm) | density of the particle (kg/m ³) | Flow rate (kg/s) | Residence time (seconds) |
|--------------|--|------------------|--------------------------|
| 1mm | 2000 | 0.005 | 173 |
| 1mm | 1800 | 0.05 | 89 |
| 5mm | 2000 | 0.005 | 3.3 |
| 5mm | 1800 | 0.05 | 513.7 |

Table 15: residence time distribution of the rectangular tank

Note: both circular tank and rectangular geometries are in reference to the thesis work submitted by Jaroslav Hanak, 2016 and Yusuf Can Emancigalo, 2016 respectively.

These results are based on **one way coupling variant** of the DPM (discrete phase model) which means the particles do not affect the fluid flow.

Here we can assess from the above tables that the residence time distribution of the conical tanks is much larger than the residence time of the circular and rectangular tanks geometries the judgement that could be made from these tables is conical tank has inlet at the bottom of the tank which is the reason why the residence time is much larger.

CHAPTER 8: CONCLUSION AND FUTURE WORK RECOMMENDATIONS

- The proposed model for the conical fish tank has been designed using ANSYS Design Modeler(18.2).
- The mesh analysis was performed by evaluating the grid convergence index using MATLAB script, but the results didn't come out well because of the unstructured mesh which cannot be perfectly similar for different mesh sizes. Another reason was that for the coarsest mesh different turbulence model was used. Still we have evaluated our simulation results with different mesh elements and different turbulence models (mostly K-epsilon and K-omega) tried to assess the velocities respectively.
- The results obtained from the simulations has been compared with the experimental data obtained from the research paper (K Lika, Journal of FISH BIOLOGY, 2015) and from (Ing.Stepan Papacek, Ph.D.).
- The average velocities over all the created planes has been evaluated and compared with the experimental data.
- The results have proven to be good but there is a possibility of manual errors involved in the calculation of velocities at different points while deploying velocimetry techniques.
- Residence time distribution of the particles (fish food) has been analyzed by employing discrete phase models in conical tank geometries and has been compared with tank geometries such as rectangular and circular.
- The results implied that the conical tank geometries have larger residence time for the particles owing to the position of the inlet being at the bottom.
- A brief literature references has been cited for more precise representation.
- The conical tank geometries have perceived to have several advantages over rectangular and circular tank geometries because it ensures better self-cleaning.
- Solution of the above work could be used as a reference for the future work by employing the same input parameters and some input parameters could be changed and analyzed.

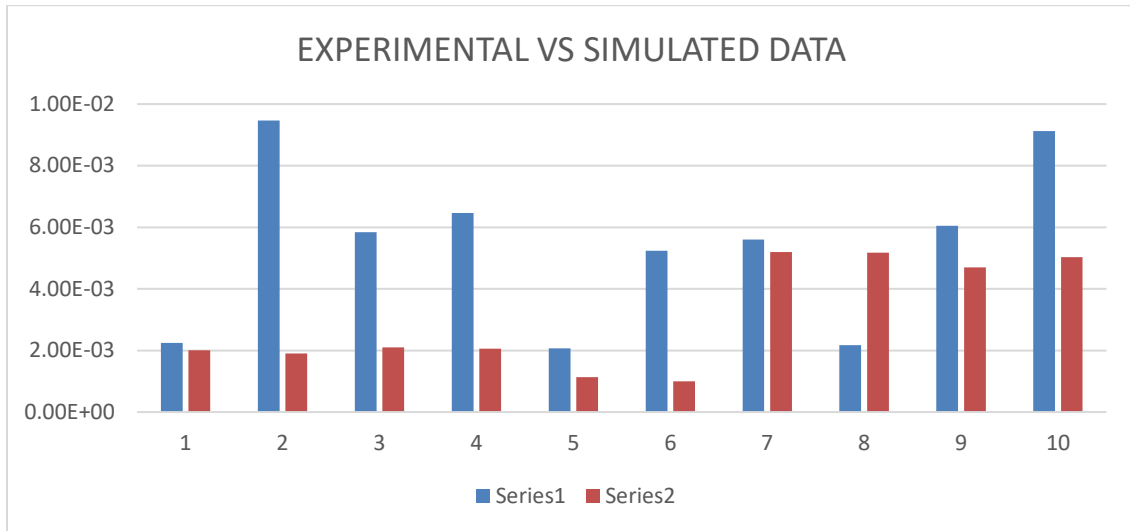
8.1: FUTURE PROSPECTS OF THE WORK

- a) As mentioned, the results have been compared for the volume of the tank 500 liters we can employ and design larger tank with much larger volume and comparison of the velocities or flow patterns can be established with the conical tank geometry, because this tank is suitable for smaller fishes breeding.
- b) A much more complicated turbulence model such as RSM (Reynolds Stress model) can be used with fine mesh which might reap better results.
- c) For better representation of the residence time we can analyze more particles with probably larger or smaller diameters and it's also imperative to know about the mechanical and physical properties of the fish feed pellets.
- d) Another future aspect of the work that could be focused on are the survival rates of the fishes in the fish tanks. These parameters completely depend upon the biology of the fishes and brief understanding of the effect of fishes on the hydrodynamics.

REFERENCES:

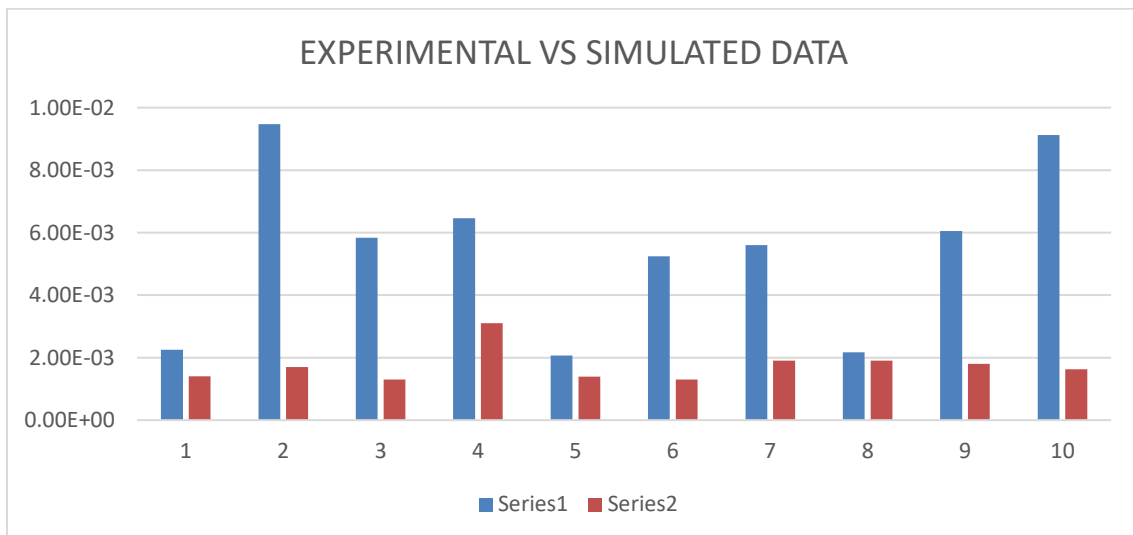
- 1) Ajay fiber glass industries [<https://www.ajayfibreglass.com.au/types/aquaculture-tanks/>]
- 2) ANSYS training materials “applications of CFD in process engineering”.
- 3) Andrew Forsythe “LAND BASED Aquaculture ASSESSMENT FRAMEWORK” [<http://www.lbaaf.co.nz/land-based-aquaculture/intensive-recirculating-aquaculture-systems-ras-/>].
- 4) Davidson, J, Summerfelt, S, 2004 “Solid removal from a cold water recirculating aquaculture system” aquaculture.
- 5) Elscolab [<http://www.elscolab.com/en/products/acoustic-doppler-velocimeter-adv>].
- 6) European Aquaculture Technology and Innovation Platform (2012). The Future of European Aquaculture. Our vision: A Strategic Agenda for Research and Innovation. Available
- 7) Esf science [<https://esfsciencenew.wordpress.com/2012/10/26/turbulent-flow-and-viscosity/>]
- 8) Jaroslav Hanak “CFD simulation of flow in fish tanks”, 2016
- 9) K. Lika M Pavlidis “Journal of FISH BIOLOGY”, 2015
- 10) Martins, C ; Eding , E; Verdeegem , M “ New developments in recirculating aquaculture systems in Europe “ , November , 2010
- 11) Odeh, M , Schrock , “ comparative hydraulics of two fisheries research circular tanks and recommendations for control of experimental bias “, Applications of Aquaculture , 2003
- 12) Pascal Klebert , Zsolt Volent “ Measurement and simulation of the three dimensional flow pattern and particle removal efficiencies flow pattern in a large floating closed sea cage with multiple inlet and drains”, November 2017.
- 13) PENTAIR INDUSTRIES, 2018, [<https://www.pentair.com/>].
- 14) Ross, RM, Wattern , BJ , “importance of rearing inlet design and stocking density to the behaviour geometries and metabolism of lake trout , 1998
- 15) Vertseeg, H K Malasekara , 1995 , “ An introduction to fluid dynamics , the Finite Element Method
- 16) Yusuf Can Emancigalou , “CFD simulation of flow in fish tank”, 2016.

APPENDICES:

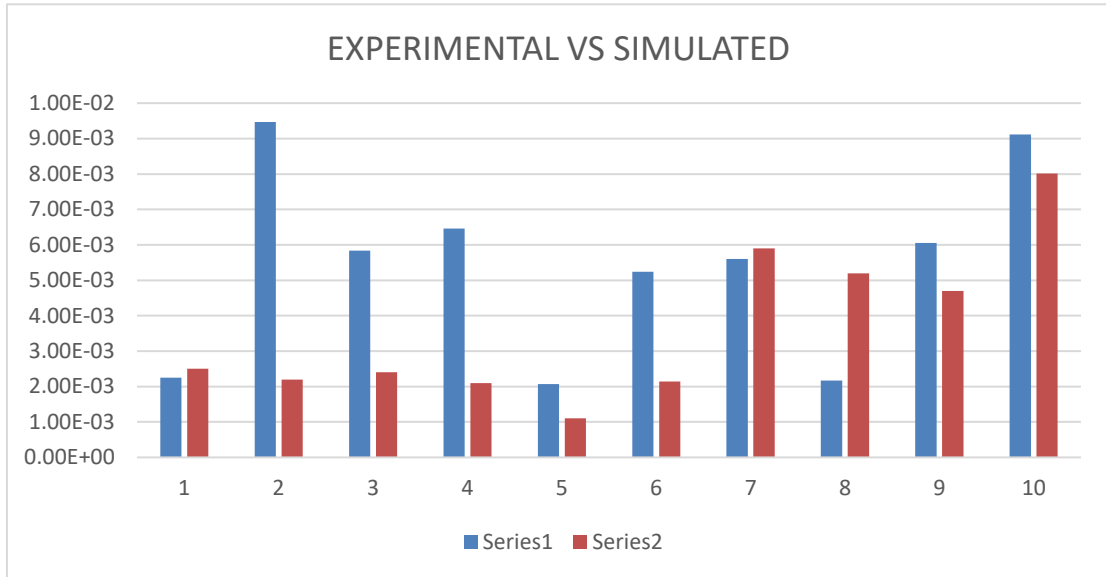


GRAPH 1 : experimental vs simulated change (k epsilon, inlet velocity 0.05 m/s, 397396 mesh elements)

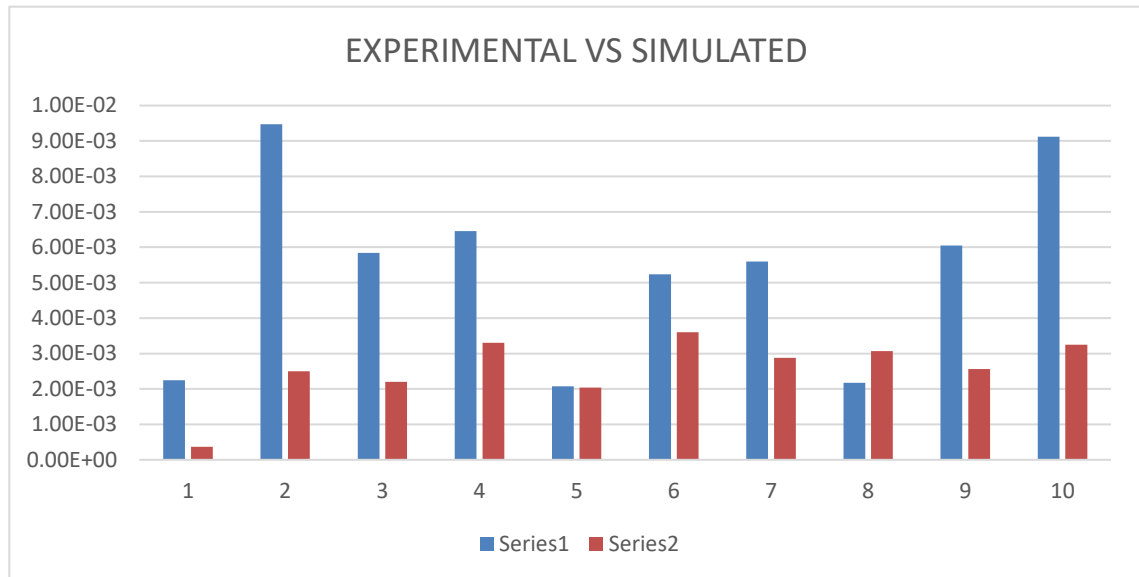
Series 1 : experimental series 2 : simulated (same for all graphs)



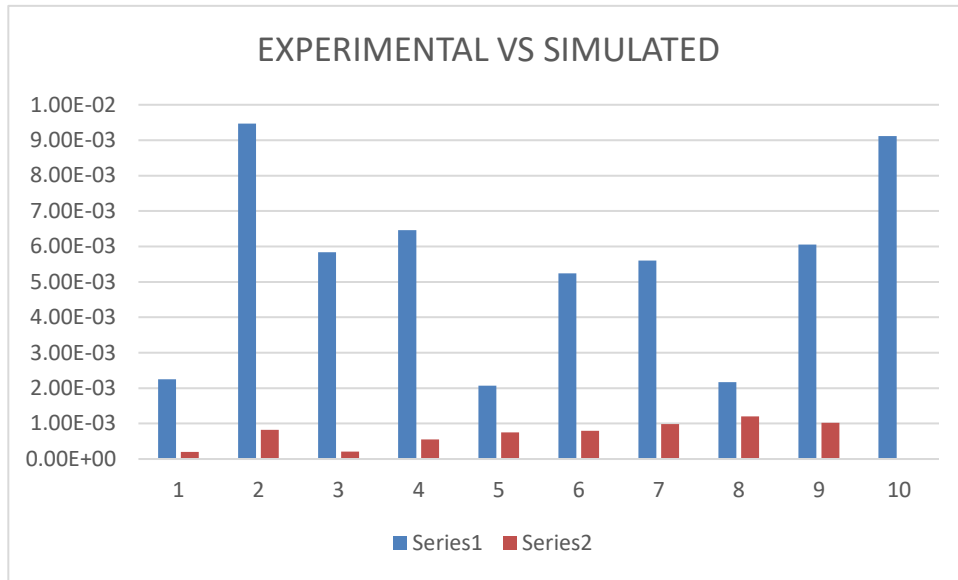
GPAPH 2: experimental vs simulated (Spallart Almaras, inlet velocity 0.05m/s)



GRAPH 3: experimental vs simulated (k epsilon realizable, inlet velocity 0.07 m/s. 900515 mesh elements)



GRAPH 4: Experimental vs simulated (k-omega 900000 mesh elements inlet velocity 0.07m/s)



GRAPH 5: Experimental vs simulated (k epsilon realizable inlet velocity 0.035 m/s)